Persistence Diagrams Estimation of Multivariate Piecewise Hölder-continuous Signals

Hugo Henneuse   HUGO.HENNEUSE@UNIVERSITE-PARIS-SACLAY.FR
Laboratoire de Mathématiques d'Orsay
Université Paris-Saclay
Orsay, 91400, France

Editor: Krishnakumar Balasubramanian

Abstract

To our knowledge, the analysis of convergence rates for persistence diagrams estimation from noisy signals has predominantly relied on lifting signal estimation results through sup-norm (or other functional norm) stability theorems. We believe that moving forward from this approach can lead to considerable gains. We illustrate it in the setting of nonparametric regression. From a minimax perspective, we examine the inference of persistence diagrams (for the sublevel sets filtration). We show that for piecewise Hölder-continuous functions, with control over the reach of the set of discontinuities, taking the persistence diagram coming from a simple histogram estimator of the signal permits achieving the minimax rates known for Hölder-continuous functions. The key novelty lies in our use of algebraic stability instead of sup-norm stability, directly targeting the bottleneck distance through the underlying interleaving. This allows us to incorporate deformation retractions of sublevel sets to accommodate boundary discontinuities that cannot be handled by sup-norm–based stability analyses.

Keywords: persistent homology, topological data analysis, geometric inference, nonparametric statistics, convergence rates

Introduction

Inferring information from noisy real-valued signals is a central subject in statistics. Specifically, in the nonparametric regression setting, where the signal is observed discretely and up to additive noise, the recovery of the whole signal structure has been extensively studied by the nonparametric statistics community. When the signal is regular (e.g., belonging to a Hölder, Sobolev, or Besov space), rigorous minimax studies and tractable optimal procedures have been provided, forming a nearly exhaustive benchmark. For an overview, see Tsybakov (2008). Nonetheless, in many practical scenarios, signals are not so regular. For instance, a photograph of a natural scene often exhibits smooth variations within homogeneous regions (such as sky, sea, or foliage), but the boundaries of the objects introduce sharp discontinuities. This has motivated the study of broader classes of irregular signals, typically signals that are only piecewise continuous. This setting has been explored in several subsequent works. We refer the reader to Qiu (2005) for an overview. However, proposed methods suffer from certain limitations: strong additional knowledge assumptions (e.g., assuming knowledge of the number of jumps, their locations, or their magnitudes), limited to low-dimensional cases (only univariate or bivariate signals), high computational costs, or lack

of rigorous and general statistical guarantees. These challenges motivate the exploration of looser descriptors that can be inferred more easily.

Over the past two decades, Topological Data Analysis (TDA) has emerged as a powerful framework, introducing geometric and topological tools to better understand complex data. Among these tools, persistent homology has received particular attention. By encoding multiscale topological features in the form of persistence diagrams (or barcodes), it provides a rich and compact summary that has proven to be a versatile descriptor, valuable from both practical and theoretical perspectives. Its applications encompass image analysis, time-series analysis, network analysis, clustering and classification tasks, and much more, as highlighted in Edelsbrunner and Harer (2008) and Chazal and Michel (2021).

A growing body of work has focused on the probabilistic and statistical analysis of persistence diagrams or related objects. Importantly, this has led to the establishment of several limit theorems (see e.g., Bubenik, 2015; Hiraoka et al., 2016; Chazal and Divol, 2018; Divol and Lacombe, 2021; Krebs and Hirsch, 2020; Krebs, 2021; Krebs and Polonik, 2025; Owada, 2022; Thomas, 2024) and descriptions of persistence diagrams (or related quantities) arising from important random objects such as Brownian motion, fractional Brownian motion, and Lévy processes (Chazal and Divol, 2018; Perez, 2020, 2022b,a), point processes (Kahle, 2009; Yogeshwaran and Adler, 2012; Chazal and Divol, 2018), and Gaussian fields (Adler et al., 2010; Bobrowski and Borman, 2012; Pranav et al., 2019; Pranav, 2021; Masoomy et al., 2021).

Beyond these asymptotic and descriptive results, another major line of research has focused on the estimation of persistence diagrams from data. In this context, the density model, in which one observes a point cloud formed by i.i.d. samples $X_1, \ldots, X_n$ from a probability distribution, has become a central framework. This line of research was initiated in a parametric setting by Bubenik and Kim (2006), and has since been extended to more general nonparametric frameworks (Chazal et al., 2011; Fasy et al., 2014; Chazal et al., 2014, 2013). These works introduce various geometric assumptions on the distribution and its support, which enable consistent recovery of persistence diagrams and quantification of convergence rates. More closely related to our setting and to signal processing, Bubenik et al. (2009) and Chung et al. (2009) tackle the problem of estimating persistence diagrams from the superlevel sets (or, equivalently, sublevel sets) in the nonparametric regression setting. In particular, in both papers, they show that a plug-in estimator based on a kernel estimate of the signal converges at rate $O((\log(n)/n)^{\alpha/(2\alpha+d)})$ over the classes of $(L, \alpha)-$Hölder signals on $\mathbb{R}^d$.

The general approach followed in all of these works involves estimating the signal or the density, quantifying the estimation error in sup-norm, Hausdorff distance, or Gromov-Hausdorff distance, and bounding the bottleneck error on the diagram using stability theorems. The power and importance of stability theorems are evident as they enable the direct translation of convergence rates in sup-norm (or similar metrics) to convergence rates in bottleneck distance over diagrams. To further emphasize the importance of stability theorems, the convergence rates derived from such results are generally minimax-optimal for regular function classes. For instance, in the density model, this has been demonstrated in Chazal et al. (2014) and Fasy et al. (2014). Similarly, in the nonparametric regression setting, although it is not explicitly stated in the original papers, the rates obtained in Bubenik et al.

2

(2009) and Chung et al. (2009) can also be shown to be minimax-optimal (see, e.g., Section 4).

However, stability-based approaches may come at the expense of generality. While persistence diagrams offer a robust summary of topological features, they encode significantly less information than the full signal. Moreover, noise does not necessarily affect persistence diagrams in the same way it impacts the raw data, meaning that sup-norm stability can sometimes obscure the diagrams' intrinsic robustness. In this direction, Turkeš et al. (2021) offers compelling empirical evidence on how common types of noise influence persistence diagrams in image analysis. Building on the idea that persistence diagrams can, in some cases, be easier to infer than the full signal, Bobrowski et al. (2017) explores this perspective in both the density estimation and nonparametric regression settings. Departing from traditional approaches, the authors propose a novel estimation method based on image persistence and show that it achieves quasi-consistency under minimal assumptions, thereby allowing for the consideration of broader function classes. We believe that these initial results highlight the necessity of moving away from sup-norm stability and, more broadly, emphasize the value of using topological or geometric descriptors when conventional nonparametric techniques yield unsatisfactory results. Nevertheless, their framework appears too broad to quantify convergence rates or even prove proper consistency, motivating the identification of more restricted function classes for which stronger and more precise results can be obtained. The present work aims to address this by studying the problem of estimating persistence diagrams in the nonparametric regression framework, over broad classes of piecewise-continuous signals. As highlighted previously, such classes of signals are ubiquitous in practical applications, particularly when dealing with image or voxel data, and estimating the full structure of these signals can be especially challenging. In such contexts, having access to descriptors, like persistence diagrams, that are easier to infer becomes particularly valuable.

Framework

Statistical model. We consider the classical nonparametric regression setting with fixed regular grid design, observing $n = N^d$ points,

$$X_i = f(x_i) + \sigma \varepsilon_i$$

with $(x_i)_{1 \leq i \leq n}$ the points of the regular grid $G_{1/N}$ over $[0,1]^d$ of step size $1/N$, σ the level of noise and $(\varepsilon_i)_{1 \leq i \leq n}$ independent standard Gaussian variables (i.e., $\mathcal{N}(0,1)$). This provides a standard and general framework for our analysis. In terms of applications, it is particularly well-suited for modeling noisy images, where the observed points correspond to pixels (or more generally, voxels) observed with additive noise.

Estimator. In this context, our goal is to estimate $\text{dgm}(f)$, the collection of persistence diagrams associated with the sublevel sets of f, by computing the diagram associated with the sublevel sets of a histogram estimator of the signal. More formally, let $h > 0$ such that Nh is an integer (and so is nh^d), consider G_h the regular orthogonal grid over $[0,1]^d$ of step h and C_h the collection of all the closed hypercubes of side h composing G_h. For all $\lambda \in \mathbb{R}$,

we define the estimator of $\mathcal{F}_\lambda = f^{-1}(]-\infty, \lambda])$ as follows:

$$\widehat{\mathcal{F}}_\lambda = \bigcup_{H \in C_{h,\lambda}} H, \text{ with } C_{h,\lambda} = \left\{ H \in C_h \text{ such that } \frac{1}{nh^d} \sum_{x_i \in H} X_i \leq \lambda \right\}.$$

the set $\widehat{\mathcal{F}}_\lambda$ represents the sublevel set indexed by λ of the histogram estimator of f and nh^d represents the cardinality of the set $H \cap G_h$ for all $H \in C_h$. Next, we consider, for all $s \in \{0, ..., d\}$, $\widehat{\mathbb{V}}_{f,s}$ the persistence module induced by the collection of homology groups:

$$\left(H_s \left(\widehat{\mathcal{F}}_\lambda \right) \right)_{\lambda \in \mathbb{R}}$$

equipped with the linear maps $\widehat{v}_\lambda^{\lambda'}$ induced by the inclusion $\widehat{\mathcal{F}}_\lambda \subset \widehat{\mathcal{F}}_{\lambda'}$, $\lambda' \geq \lambda$. We define $\widehat{\text{dgm}(f)}$ as the associated collection of persistence diagrams. A natural question is how to calibrate the window size h for signals. From the proof of Lemma 7 (Appendix B.1), a good choice is taking h such that

$$h^\alpha > \sqrt{\frac{\log(1/h^d)}{nh^d}} \tag{1}$$

thus, we can choose:

$$h \asymp \left(\frac{\log(n)}{n} \right)^{\frac{1}{d+2\alpha}}.$$

Regularity assumptions. To avoid excessive technicalities, the detailed presentation of the assumptions on the function f considered in this work is deferred to Section 2 (see Assumptions **A0**–**A3**). The class of functions satisfying these assumptions is denoted by $S_d(M, L, \alpha, R)$ and consists essentially of piecewise (L, α)-Hölder continuous functions, uniformly bounded by M, whose pieces have boundaries with reach (an important geometric measure; see Section 2) bounded below by R.

Contributions

In this framework, we study the convergence properties of the estimator $\widehat{\text{dgm}(f)}$ with respect to the bottleneck distance over the classes $S_d(M, L, \alpha, R)$. Our analysis departs from approaches based on sup-norm stability by instead leveraging a weaker notion of stability, known as the algebraic stability theorem (Chazal et al., 2009), which allows us to upper-bound the bottleneck distance between the estimated and true persistence diagrams via an interleaving of the underlying persistence modules (see Section 1). The core of our approach is then to construct such an interleaving by exploiting key geometric properties of the sublevel sets, notably through the use of deformation retractions (see Section 3, p. 13, for a detailed outline). This enables us to handle discontinuities that typically cause sup-norm–based approaches to fail. The main consequence of this analysis is the following upper bound over the rates of convergence of $\widehat{\text{dgm}(f)}$:

Theorem 2

$$\sup_{f \in S_d(M,L,\alpha,R)} \mathbb{E} \left(d_b \left(\widehat{\text{dgm}(f)}, \text{dgm}(f) \right) \right) \lesssim \left(\frac{\log(n)}{n} \right)^{\frac{\alpha}{d+2\alpha}}.$$

4
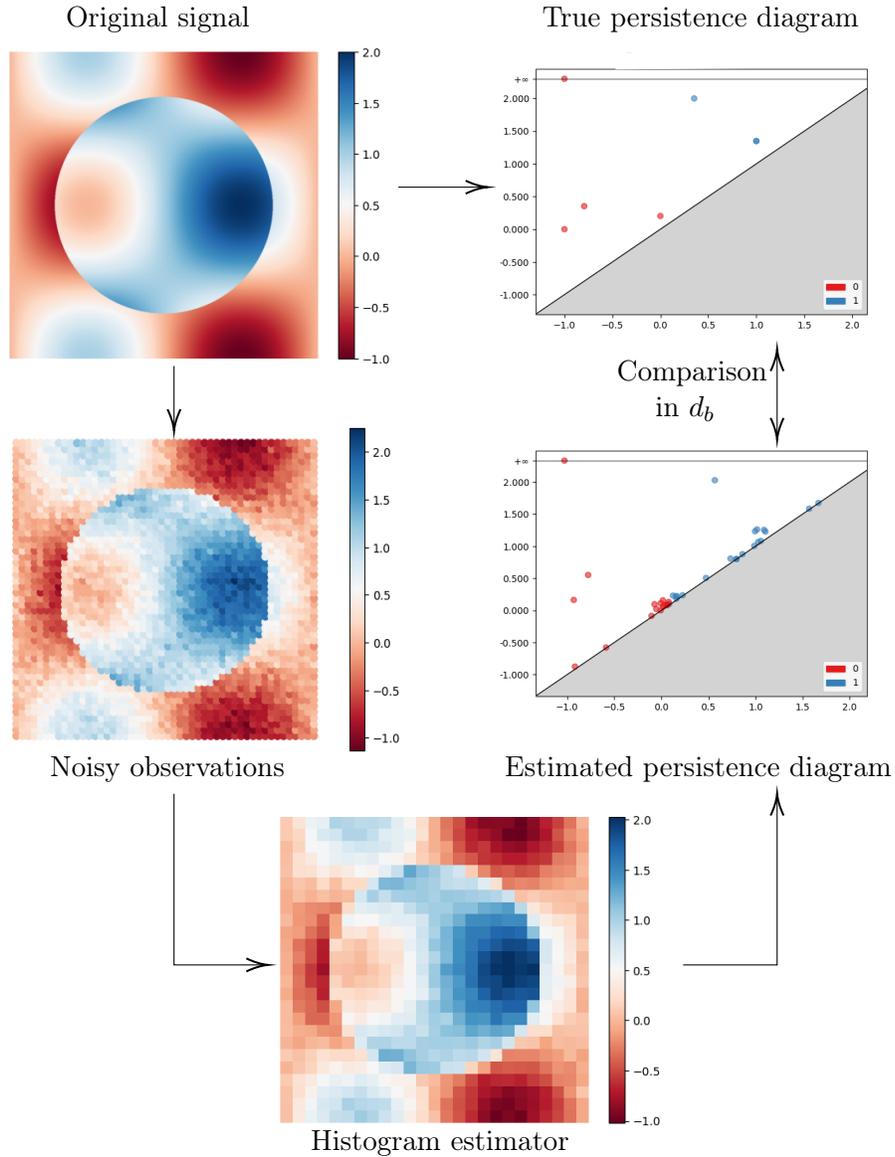
Figure 1: Numerical illustration of the estimation procedures for $f(x,y) = \cos(2\pi x)\sin(2\pi x) + \mathbf{1}_{(x-1/2)^2+(y-1/2)^2<1/8}$, $\sigma = 0.1$, $n = 2500$, $h = 1/4(\frac{\log(n)}{n})^{1/4}$.

Furthermore, we establish that these rates are optimal, in the minimax sense, over the classes $S_d(M, L, \alpha, R)$.

Theorem 3

$$\inf_{\widehat{\mathrm{dgm}(f)}} \quad \sup_{f \in S_d(M,L,\alpha,R)} \quad \mathbb{E}\left(d_b\left(\widehat{\mathrm{dgm}(f)}, \mathrm{dgm}(f) \right) \right) \gtrsim \left(\frac{\log(n)}{n} \right)^{\frac{\alpha}{d+2\alpha}}.$$

Interestingly, these rates coincide with the rates for Hölder spaces, obtained in Corollary 4.4 of Bubenik et al. (2009). This means that, up to a multiplicative constant, there is no additional cost to consider signals in $S_d(M, L, \alpha, R)$. It demonstrates the gain of breaking free from the usual analysis approach in TDA and the robustness to discontinuities of persistence diagram estimation. Furthermore, as such irregularities are challenging to handle for signal estimation, these results promote the use of persistence diagrams while processing noisy (irregular) signals. It is also worth noting that our analysis can be readily extended to other popular statistical models, as illustrated in the context of the Gaussian white noise model in Appendix D.

Organization

The paper is organized as follows. Section 1 provides some background on persistent homology. Section 2 details the regularity assumptions on f. Section 3 is dedicated to the proof of Theorem 2. Section 4 is dedicated to the proof of Theorem 3. Section 5 provides some numerical illustrations of our results in the context of image analysis. Appendix A,B, and C contain proofs of technical lemmas, propositions, and claims invoked in this paper. Appendix D presents an extension of our results to the Gaussian white noise model.

1. Topological Background

This section aims to provide the essential topological background needed to follow this paper.

1.1 Homology and Invariance under Deformation Retraction

We provide a brief introduction to (singular) homology, emphasizing key properties that are central to our work. For further details, we refer the reader to Hatcher (2000), which inspired this section. We begin by introducing the notion of singular simplex.

Definition 1 *Let a topological space X and Δ^s the standard $s-$simplex (i.e., the simplex of dimension s whose vertices are the $s+1$ standard unit vectors in $\mathbb{R}^{s+1}$, denoted $v_1, ..., v_s$). A singular $s-$simplex of X is a continuous map $\sigma : \Delta^s \to X$.*

Singular simplices are continuous maps from a standard simplex to the space X. They are not required to be homeomorphisms of any kind and can be widely singular, which allows for very general construction of homology groups. From these singular simplices, we can define the space of singular chains and the boundary operator.

Definition 2 *The group of $s-$chains on X, $C_s(X)$, for a field $\mathbb{K}$, is the abelian group of finite formal sums $\sum_i c_i \sigma_i$ with σ_i a singular s-simplex of X and $c_i \in \mathbb{K}$.*

Definition 3 *The boundary $\partial_s \sigma$ of a s-singular simplex σ is defined by:*

$$\partial_s \sigma = \sum_{i=0}^{s} (-1)^i \sigma|_{[v_0,\cdots,\widehat{v_i},\cdots,v_s]}.$$

where $[v_0,\cdots,\hat{v}_i,\cdots,v_s] = [v_0,\cdots,v_{i-1},v_{i+1},\cdots,v_s]$. The map $\sigma|_{[v_0,\cdots,\hat{v}_i,\cdots,v_s]}$ can then be thought of as a map from Δ^{s-1} to X. The boundary operator $\partial_s : C_s(X) \to C_{s-1}(X)$ is then defined by:

$$\partial_s : C_s(\mathcal{K}) \to C_{s-1}(\mathcal{K})$$
$$c = \sum_i c_i \sigma_i \to \partial_s c = \sum_i c_i \partial_s \sigma_i.$$

A crucial property of the boundary operator is that applying it twice always gives zero: $\partial_s \circ \partial_{s+1} = 0$. We can then consider two subgroups of $C_s(X)$:

- the $s-$cycles: $Z_s = \mathrm{Ker}(\partial_s)$, i.e., the s-chains whose boundary is zero.

- the $s-$boundaries: $B_s = \mathrm{Im}(\partial_{s+1})$ i.e., the $s-$chains that are themselves boundaries of higher-dimensional chains.

As $\partial_s \circ \partial_{s+1} = 0$, B_s is a normal subgroup of Z_s. We can then define the $s-$th homology groups as $s-$cycles quotiented by $s-$boundaries.

Definition 4 *Let X be a topological space and $s \in \mathbb{N}$. We can define the $s-$th (singular) homology group of $\mathcal{K}$ (on the field $\mathbb{K}$) by:*

$$H_s(X) = Z_s/B_s$$

Intuitively, these groups identify the "holes" in the space X at a given dimension: $H_0(X)$ identifies its connected components, $H_1(X)$ its loops, $H_2(X)$ its enclosed cavities, and so on.

A key property of homology, which we extensively exploit in this work, is that it is invariant under deformation retraction, meaning that if a space can be continuously "shrunk" to a subspace without tearing or gluing, its homology groups remain the same. The construction of such deformations is a classical technique that lies at the heart of many foundational results in algebraic topology.

Definition 5 *A subspace A of X is called a deformation retract of X if there is a continuous $F : X \times [0,1] \to X$ such that for all $x \in X$ and $a \in A$,*

- $F(x,0) = x$

- $F(x,1) \in A$

- $F(a,1) = a$.

The function F is then called a (deformation) retraction from X to A.

A deformation retraction F from X to A ensures that X and A are "homotopy equivalent" (see Hatcher, 2000, pages 2–3), and thus are topologically similar. In particular, F induces isomorphisms between the homology groups of X and A. More precisely, for all $t \in [0,1]$, $F(.,t)$ induces a group morphism $F^{\#}(.,t) : C_s(X) \to C_S(X)$ between $s-$chains of X defined by composing each singular s-simplex $\sigma : \Delta^s \to X$ with $F(.,t)$ to get a singular s-simplex $F^{\#}(\sigma,t) = F(.,t) \circ \sigma : \Delta^s \to X$, then extending $F^{\#}(.,t)$ linearly via $F^{\#}\left(\sum_i n_i \sigma_i, t\right) = \sum_i n_i F^{\#}(\sigma_i, t) = \sum_i n_i F(.,t) \circ \sigma_i$. The group morphism $F^*(.,t) : H_s(X) \to H_s(X)$ defined by $[C] \mapsto [F^{\#}(C,t)]$ can be shown to be an isomorphism for all $t \in [0,1]$ (see Hatcher, 2000, pages 110-113). In particular, $F^*(.,1) : H_s(X) \to H_s(A)$ is an isomorphism.

1.2 Filtrations, Persistence Modules and Diagrams

The idea behind persistent homology is to encode the evolution of the topology (in the homology sense) of a nested family of topological spaces, called a filtration. As we move along indices, topological features (connected components, cycles, cavities, ...) can appear or disappear (existing connected components merge, cycles or cavities are filled, ...). Two keys to formalize this idea, which we use throughout this paper, are the notions of filtration and of persistence module.

Definition 6 *Let $\Lambda \subset \mathbb{R}$ be a set of indices. A filtration indexed by Λ is a family $(\mathcal{K}_\lambda)_{\lambda \in \Lambda}$ of topological spaces satisfying, for all $\lambda, \lambda' \in \Lambda, \lambda \leqslant \lambda'$*

$$\mathcal{K}_\lambda \subset \mathcal{K}_{\lambda'}.$$

The typical filtration that we will consider in this paper is, for a function $f : \mathbb{R}^d \to \mathbb{R}$, the family of sublevel sets $(\mathcal{F}_\lambda)_{\lambda \in \mathbb{R}} = \left(f^{-1}(]-\infty, \lambda])\right)_{\lambda \in \mathbb{R}}$.

Definition 7 *Let $\Lambda \subset \mathbb{R}$ be a set of indices. A persistence module over Λ is a family $\mathbb{V} = (\mathbb{V}_\lambda)_{\lambda \in \Lambda}$ of vector spaces equipped with linear maps $v_\lambda^{\lambda'} : \mathbb{V}_\lambda \to \mathbb{V}_{\lambda'}$ such that, for all $\lambda \leqslant \lambda' \leqslant \lambda'' \in \Lambda$,*

$$v_\lambda^\lambda = id$$

and

$$v_{\lambda'}^{\lambda''} \circ v_\lambda^{\lambda'} = v_\lambda^{\lambda''}.$$

The typical persistence module that we will consider in this paper is, for a function $f : \mathbb{R}^d \to \mathbb{R}$ and $s \in \mathbb{N}$, the family of homology groups $\mathbb{V}_{f,s} = (H_s(\mathcal{F}_\lambda))_{\lambda \in \mathbb{R}}$ equipped with $v_\lambda^{\lambda'}$ the linear maps induced by the inclusion $\mathcal{F}_\lambda \subset \mathcal{F}_{\lambda'}$. To be more precise, in this paper, $H_s(.)$ is the singular homology functor in degree s with coefficients in a field (typically $\mathbb{Z}/2\mathbb{Z}$). Hence, $H_s(\mathcal{F}_\lambda)$ is a vector space.

Under the q-tameness assumption (see Definition 10 in Appendix A), a persistence module $\mathbb{V}$ can be fully described by a multi-set in $\mathbb{R}^2$, known as its persistence diagram:

$$\text{dgm}(\mathbb{V}) = \{(b_j, d_j) \mid j \in J\} \subset \overline{\mathbb{R}}^2.$$

In this representation, each b_j represents the birth time of a topological feature (e.g., the emergence of a connected component or the formation of a cycle), while d_j represents its death time (e.g., the merging of two components or the filling of a cycle). The difference

$d_j - b_j$ corresponds to the feature's lifetime. For a detailed construction of persistence diagrams, we refer the reader to Chazal et al. (2016). In cases where we consider the collection of modules $(\mathbb{V}_{f,s})_{s \in \mathbb{N}}$ associated with the sublevel sets filtration of f, we denote by $\mathrm{dgm}(f)$ the collection of associated persistence diagrams.

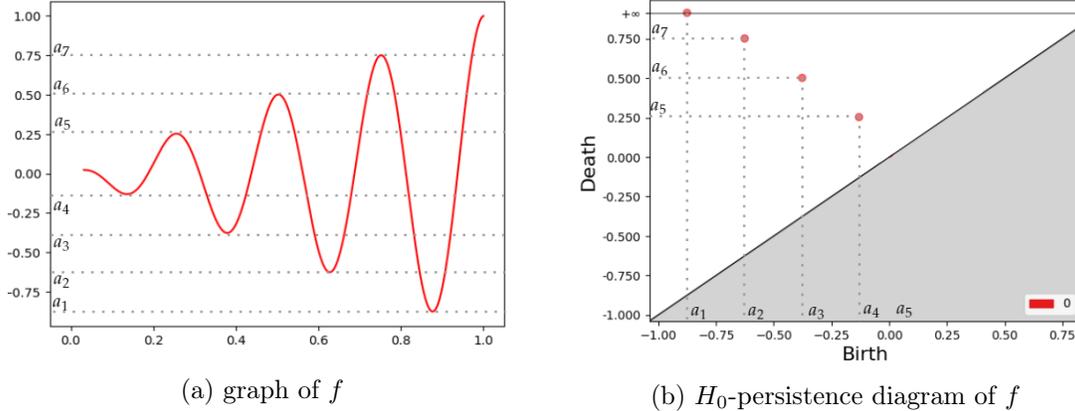(a) graph of f (b) H_0-persistence diagram of f

Figure 2: Graph of $f(x) = x \cos(8\pi x)$ over $[0, 1]$ and the (0-th) persistence diagram associated to its sublevel sets filtration. a_1, ..., a_4 correspond to local minima of f and thus birth times in $\mathrm{dgm}(f)$. a_5, ..., a_7 correspond to local maxima of f and thus death times in $\mathrm{dgm}(f)$.

1.3 Bottleneck Distance, Interleaved Modules and Algebraic Stability

To compare persistence diagrams, we need a distance. A popular such distance, due to its stability properties, is the bottleneck distance. This distance is defined as the infimum over all matchings between points in diagrams of the maximal sup norm distance between two matched points. To allow for matchings between diagrams that do not contain the same number of points, the diagonal is added to the diagrams. This distance will be used in this work to evaluate the quality of our estimation procedures.

Definition 8 *The bottleneck distance between two persistence diagrams D_1 and D_2 is,*

$$d_b(D_1, D_2) = \inf_{\gamma \in \Gamma} \sup_{p \in D_1 \cup \Delta} ||p - \gamma(p)||_\infty$$

with Γ the set of all bijections between $D_1 \cup \Delta$ and $D_2 \cup \Delta$, where $\Delta = \{(x, x), x \in \mathbb{R}\}$.

Another notion that will be the key to proving our upper bounds is the notion of interleaving between persistence modules. We use in particular the fact that if two modules are $\varepsilon-$interleaved, then the bottleneck distance between their diagrams is upper bounded by ε in bottleneck distance.

Definition 9 *Two persistence modules $\mathbb{V} = (\mathbb{V}_\lambda)_{\lambda \in I \subset \mathbb{R}}$ and $\mathbb{W} = (\mathbb{W}_\lambda)_{\lambda \in I \subset \mathbb{R}}$ are said to be ε-interleaved if there exist two families of linear maps, which we will refer to as (persistence module) morphisms:*

$$\phi = (\phi_\lambda : \mathbb{V}_\lambda \to \mathbb{W}_{\lambda+\varepsilon})_{\lambda \in I \subset \mathbb{R}} \ \ and \ \ \psi = (\psi_\lambda : \mathbb{W}_\lambda \to \mathbb{V}_{\lambda+\varepsilon})_{\lambda \in I \subset \mathbb{R}}$$
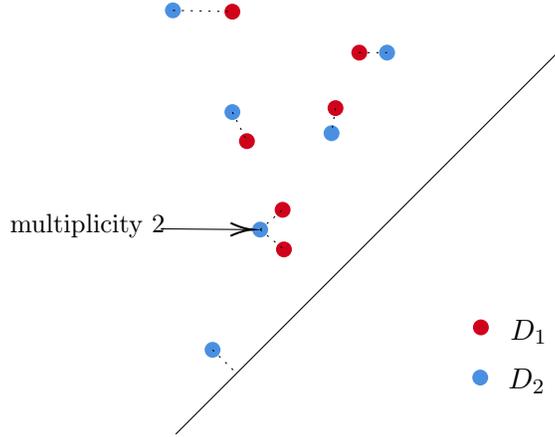
Figure 3: Optimal matching for the bottleneck distance between D_1 and D_2.

such that, for all $\lambda < \lambda'$, the following diagrams commutes,

Theorem (algebraic stability (Chazal et al., 2009)) *Let $\mathbb{V}$ and $\mathbb{W}$ be two $q-$tame persistence modules (see definition 10 in Appendix A). If $\mathbb{V}$ and $\mathbb{W}$ are $\varepsilon-$interleaved then,*

$$d_b\left(\mathrm{dgm}(\mathbb{V}), \mathrm{dgm}(\mathbb{W})\right) \leq \varepsilon$$

Note that in the context of sublevel set persistence, a direct consequence of this theorem is the stability of persistence diagrams with respect to the sup-norm distance between functions. More precisely, if two q-tame real-valued functions f and g satisfy $\|f - g\|_\infty \leq \varepsilon$, then their sublevel sets filtrations satisfy

$$\mathcal{F}_{\lambda-\varepsilon} \subset \mathcal{G}_\lambda \subset \mathcal{F}_{\lambda+\varepsilon}, \quad \text{for all } \lambda \in \mathbb{R}.$$

The linear maps induced in homology by these inclusions define an ε-interleaving. By the algebraic stability theorem, this implies:

$$d_b(\mathrm{dgm}(f), \mathrm{dgm}(g)) \leq \varepsilon.$$

10

2. Regularity Assumptions

We here detail and discuss the regularity assumptions on f mentioned in the Introduction. For a set $A \subset [0,1]^d$, we denote $\overline{A}$ its closure, A° its interior, ∂A its boundary and A^c its complement. Let $f : [0,1]^d \to \mathbb{R}$, we make the following assumptions about f:

A0. f is bounded by M, i.e., for all $x \in [0,1]^d$, $|f(x)| \le M$.

A1. f is a piecewise $(L, \alpha)-$Hölder-continuous function, i.e., there exist $M_1, ..., M_l$ disjoint open sets of $[0,1]^d$ such that

$$\bigcup_{i=1}^{l} \overline{M_i} = [0,1]^d$$

and for all $i \in \{1, ..., l\}$ and $x, y \in M_i$,

$$|f(x) - f(y)| \le L\|x - y\|_2^\alpha.$$

A2. f satisfies, for all $x_0 \in [0,1]^d$,

$$\liminf_{x \in \bigcup_{i=1}^{l} M_i \to x_0} f(x) = f(x_0)$$

In this context, two signals, differing only on a null set, are statistically indistinguishable. Persistent homology is sensitive to point-wise irregularity. As a result, two signals differing only on a null set can have very different persistence diagrams. Assumption **A2** prevents such scenarios. Furthermore, note that for any piecewise Hölder-continuous function f, there exists a modification $\tilde{f}$ satisfying Assumption **A2** such that f and $\tilde{f}$ coincide except on a set of measure zero. Following this remark, note that, although this assumption is necessary for the proofs of our main results, it is more of a convention to avoid statistical indistinguishability than a true limitation, at least from a practical perspective.

A3. $\bigcup_{i=1}^{l} \partial M_i \cap]0,1[^d$ is a $C^{1,1}$ hypersurface, and, for $R > 0$, it satisfies:

$$\text{reach}\left(]0,1[^d \cap \bigcup_{i=1}^{l} \partial M_i\right) \ge R \text{ and } d_2\left(\bigcup_{i=1}^{l} \partial M_i \cap]0,1[^d, \partial [0,1]^d\right) \ge R$$

where, for a set $A \subset \mathbb{R}^d$, $\text{reach}(A) =$

$$\sup\left\{r \in \mathbb{R} : \forall x \in \mathbb{R}^d \backslash A \text{ with } d_2(\{x\}, A) < r, \exists! y \in A \text{ s.t. } \|x - y\|_2 = d_2(\{x\}, A)\right\}$$

and,

$$d_2(A, B) = \max\left(\sup_{x \in B} \inf_{y \in A} \|x - y\|_2, \sup_{x \in A} \inf_{y \in B} \|x - y\|_2\right).$$

is the Hausdorff distance between two sets A and B. The reach is a curvature measure introduced by Federer (1959). An intuitive way to understand it is that if A has a reach R, we can roll a ball of radius R along the boundary of A. Positive reach assumptions

are fairly common in statistical TDA (Balakrishnan et al., 2012; Niyogi et al., 2008) and geometric inference (Genovese et al., 2012; Kim et al., 2016; Aamari and Levrard, 2017; Aamari et al., 2019; Berenfeld et al., 2021). Here, the first part of Assumption **A3** ensures geometric control over the union of the boundary of the M_i, $i \in \{1, ..., l\}$, in the interior of $[0,1]^d$, for example, it prevents the appearance of cusps, corners, and multiple points. The second part ensures that discontinuities do not appear too close to the boundary of the cube $[0,1]^d$.

(a) Assumption **A3** verified   (b) Assumption **A3** not verified
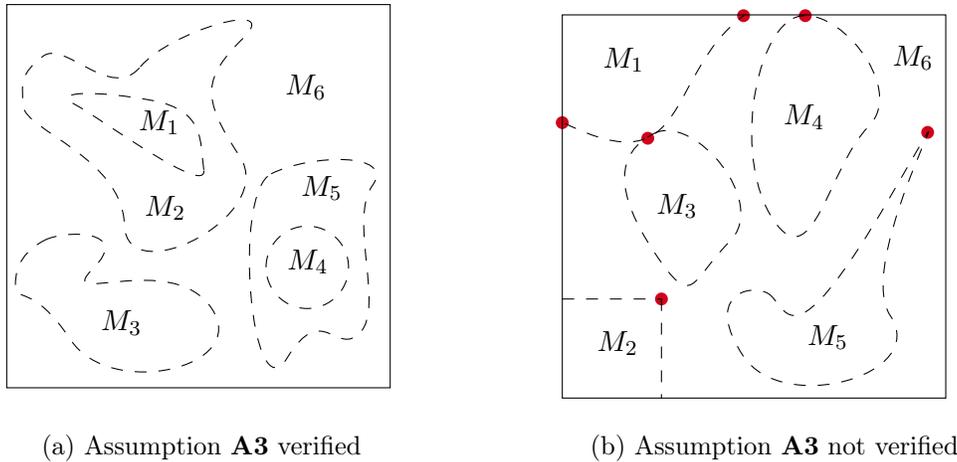
Figure 4: Illustration of Assumption **A3**

We denote $S_d(M, L, \alpha, R)$ the set of such functions. The combination of Assumptions **A1**, **A2** and **A3** ensures that the persistence diagrams of $f \in S_d(M, L, \alpha, R)$ are well-defined (see Appendix A, Proposition 1).

3. Upper Bounds

This section is devoted to the proof of Theorem 2. First, we introduce some notations. For a point $x \in [0,1]^d$ and $b > 0$, we denote the closed Euclidean ball centered at x of radius b:

$$B_2(x, b) = \{y \in [0,1]^d, ||x - y||_2 \le b\}$$

Similarly, for a set $A \subset \mathbb{R}^d$ and $b \ge 0$, we denote,

$$A^b = B_2(A, b) = \left\{ x \in [0,1]^d \text{ s.t. } d_2(\{x\}, A) \le b \right\}$$

and

$$A^{-b} = \left((A^c)^b \right)^c.$$

We also define, for all $h > 0$:

$$N_h = \frac{\max\limits_{H \in C_h} \left| \frac{\sigma}{nh^d} \sum\limits_{x_i \in H} \varepsilon_i \right|}{\sqrt{2\sigma^2 \frac{\log(1/h^d)}{nh^d}}}.$$

Proof outline. The strategy is to construct an interleaving between the estimated and true persistence modules and then apply the algebraic stability theorem (Chazal et al., 2009). To do so, we need to construct two families of linear maps ϕ and ψ (i.e., module morphisms):

$$\mathbb{V}_{f,s} \xrightarrow{\phi} \widehat{\mathbb{V}}_{f,s} \xrightarrow{\psi} \mathbb{V}_{f,s}$$

satisfying Definition 9. The outline of our proof is as follows:

- We show in Lemma 1 that for some $\beta_1 \geq 0$, depending on N_h, $\widehat{\mathcal{F}}_\lambda \subset \mathcal{F}_{\lambda+\beta_1 h^\alpha}^{\sqrt{d}h}$, which induces a linear map from the homology group of $\widehat{\mathcal{F}}_\lambda$ to the homology group of $\mathcal{F}_{\lambda+\beta_1 h^\alpha}^{\sqrt{d}h}$.

- We identify in Lemma 2 two families of sets $(\mathcal{K}_\lambda)_{\lambda \in \mathbb{R}}$ and $(\mathcal{G}_\lambda)_{\lambda \in \mathbb{R}}$ such that for some $\beta_2, \beta_3 \geq 0$, depending on N_h, $\mathcal{F}_{\lambda+\beta_1 h^\alpha}^{\sqrt{d}h} \subset \mathcal{K}_{\lambda+\beta_2 h^\alpha}$, $\mathcal{K}_{\lambda+\beta_2 h^\alpha}$ (deformation) retracts onto $\mathcal{G}_{\lambda+\beta_2 h^\alpha}$ and $\mathcal{G}_{\lambda+\beta_2 h^\alpha} \subset \mathcal{F}_{\lambda+\beta_3 h^\alpha}$ which induces a linear map from the homology group of $\mathcal{F}_{\lambda+\beta_1 h^\alpha}^{\sqrt{d}h}$ to the homology group of $\mathcal{F}_{\lambda+\beta_3 h^\alpha}$.

- The composition of the two linear maps obtained previously induces a linear map from the homology group of $\widehat{\mathcal{F}}_\lambda$ to the homology group of $\mathcal{F}_{\lambda+\beta_3 h^\alpha}$. This is (essentially) our ϕ.

- We proceed similarly to construct ψ, identifying in Lemma 3 two families $(\mathcal{N}_\lambda)_{\lambda \in \mathbb{R}}$ and $(\mathcal{M}_\lambda)_{\lambda \in \mathbb{R}}$ such that for some $\beta_4, \beta_5 \geq 0$, depending on N_h, $\mathcal{F}_\lambda \subset \mathcal{N}_{\lambda+\beta_4 h^\alpha}$, $\mathcal{N}_{\lambda+\beta_4 h^\alpha}$ (deformation) retracts onto $\mathcal{M}_{\lambda+\beta_4 h^\alpha}$ and $\mathcal{M}_{\lambda+\beta_4 h^\alpha} \subset \mathcal{F}_{\lambda+\beta_5 h^\alpha}^{-\sqrt{d}h}$. Moreover, in Lemma 1 we show that for some $\beta_6 \geq 0$, depending on N_h, $\mathcal{F}_{\lambda+\beta_5 h^\alpha}^{-\sqrt{d}h} \subset \widehat{\mathcal{F}}_{\lambda+\beta_6 h^\alpha}$.

- We prove in Lemma 4 that the supports of these retractions, when applied to $x \in \widehat{\mathcal{F}}_\lambda$, remain within $\widehat{\mathcal{F}}_{\lambda+\beta_7 h^\alpha}$, for some $\beta_7 \geq 0$. Then, we use this additional property to show that the ϕ and ψ we construct satisfy Definition 9 and define an interleaving that depends on N_h.

- We conclude using a standard concentration argument on N_h (Lemma 5).

Following this outline, we formally state Lemmas 1-5, which form the fundamental building blocks of our proof.

Lemma 1 *Let $f : [0,1]^d \to \mathbb{R}$. For all $\lambda \in \mathbb{R}$ and $h > 0$ satisfying (1),*

$$\mathcal{F}_{\lambda-\sqrt{2}\sigma N_h h^\alpha}^{-\sqrt{d}h} \subset \widehat{\mathcal{F}}_\lambda \subset \mathcal{F}_{\lambda+\sqrt{2}\sigma N_h h^\alpha}^{\sqrt{d}h}.$$

The proof of Lemma 1 is provided in Appendix B.1. This double inclusion induces a morphism from $(H_s(\mathcal{F}_\lambda^{-\sqrt{d}h}))_{\lambda \in \mathbb{R}}$ to $\widehat{\mathbb{V}}_{f,s}$ and a morphism from $\widehat{\mathbb{V}}_{f,s}$ to $(H_s(\mathcal{F}_\lambda^{\sqrt{d}h}))_{\lambda \in \mathbb{R}}$.

Now, what we need to construct the desired interleaving is, for arbitrary $h > 0$:

- a morphism from $\mathbb{V}_{f,s}$ to $(H_s(\mathcal{F}_\lambda^{-h}))_{\lambda \in \mathbb{R}}$

- a morphism from $(H_s(\mathcal{F}_\lambda^{h}))_{\lambda \in \mathbb{R}}$ to $\mathbb{V}_{f,s}$

13

We begin with the construction of the morphism from $(H_s(\mathcal{F}_\lambda^h))_{\lambda \in \mathbb{R}}$ to $\mathbb{V}_{f,s}$. The main difficulty arises near the boundaries of the regular pieces. When we thicken $\mathcal{F}_\lambda$ by h, the resulting set $\mathcal{F}_\lambda^h$ may extend into regions where the signal is significantly larger than λ. This prevents us from establishing a straightforward inclusion of the form:

$$\mathcal{F}_\lambda^h \subset \mathcal{F}_{\lambda+\varepsilon}$$

for a reasonable ε. In particular, this is why standard techniques based on sup-norm stability cannot be directly applied in this setting.

To formalize this issue, we define the set of problematic points as

$$S_{\lambda,h} = \left(\left(\bigcup_{i=1}^l \partial M_i \cap]0,1[^d \right)^h \setminus \mathcal{F}_{\lambda+Lh^\alpha} \right) \cap \mathcal{F}_\lambda^h.$$

Intuitively, $S_{\lambda,h}$ consists of the regions where $\mathcal{F}_\lambda^h$ extends beyond $\mathcal{F}_{\lambda+Lh^\alpha}$, preventing a controlled inclusion. Our goal is to smoothly "push" these points into $\mathcal{F}_{\lambda+\varepsilon}$ for some $\varepsilon \asymp h^\alpha$. To achieve this, we will construct a deformation retraction using Theorem 4.8 of Federer (1959). Under Assumption **A3**, this theorem guarantees that for every $x \in [0,1]^d$ at a (Euclidean) distance strictly smaller than R from $]0,1[^d \cap \bigcup_{i=1}^l \partial M_i$, there exists a unique closest point in $]0,1[^d \cap \bigcup_{i=1}^l \partial M_i$, denoted by $\xi(x)$, i.e., there exists a well-defined projection map. Moreover, the function ξ is continuous.

Using Assumptions **A1** and **A2**, we can show (see the proof of Lemma 2) that for all $x \in S_{\lambda,h}$, the projection $\xi(x)$ belongs to $\mathcal{F}_{\lambda+\varepsilon}$ for some $\varepsilon \asymp h^\alpha$. The idea is then to map each point $x \in S_{\lambda,h}$ to $\xi(x)$, moving along the line segment $[x, \xi(x)]$. However, turning this idea into a proper deformation retraction requires several technical adjustments.

The first issue is that the segments $[x, \xi(x)]$ for $x \in S_{\lambda,h}$ may not be contained entirely in $\mathcal{F}_\lambda^h$. To resolve this, we consider a slightly larger set, adding the segments $[x, \xi(x)]$ for all $x \in S_{\lambda,h}$:

$$\mathcal{K}_{\lambda,h} := \mathcal{F}_\lambda^h \cup \left(\bigcup_{x \in S_{\lambda,h}} [x, \xi(x)] \right) \subset \mathcal{F}_\lambda^{2h}.$$

Additionally, to ensure the continuity of the deformation retraction, we must avoid moving excessively points of $\bigcup_{x \in S_{\lambda,h}} [x, \xi(x)] \cap M_i$ that are close to $\mathcal{F}_{\lambda+Lh^\alpha} \cap M_i$ for all $i \in \{1, \ldots, l\}$. To achieve this, we introduce the condition (**C1**): there exists some $i \in \{1, \ldots, l\}$ such that

$$x \in \bigcup_{x \in S_{\lambda,h}} [x, \xi(x)] \cap M_i \tag{2}$$

and

$$d_2\left(\xi(x), M_i \cap \mathcal{F}_{\lambda+Lh^\alpha}\right) \geq 2h - ||x - \xi(x)||_2. \tag{3}$$

We then define the function $F_{\lambda,h} : \mathcal{K}_{\lambda,h} \times [0,1] \to \mathcal{K}_{\lambda,h}$, which will serve as our deformation retraction, by:

$$F_{\lambda,h}(x) = \begin{cases} (1-t)x + t\left(\xi(x) + (2h - d_2\left(\xi(x), M_i \cap \mathcal{F}_{\lambda+Lh^\alpha}\right))_+ \frac{x - \xi(x)}{||x - \xi(x)||_2}\right), & \text{under } (\mathbf{C1}), \\ x, & \text{otherwise.} \end{cases}$$
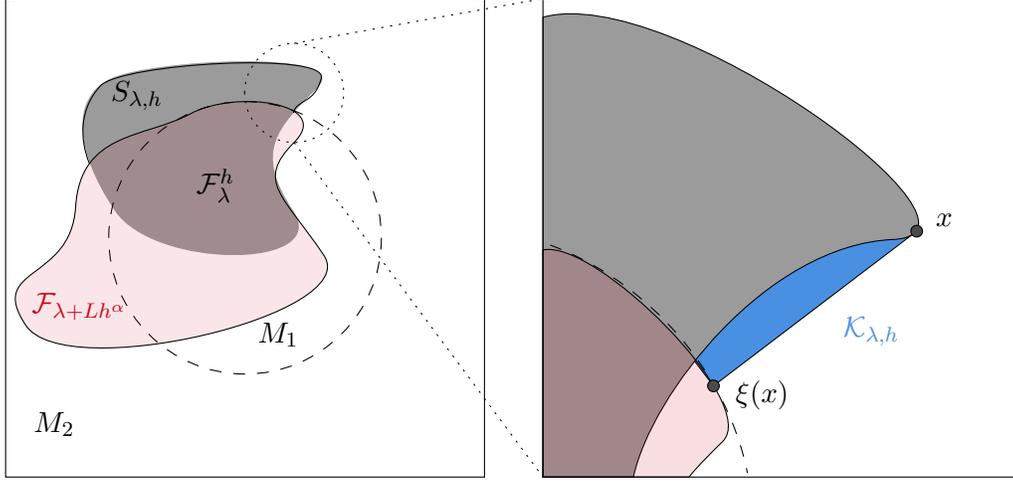
Figure 5: Illustration of the sets $\mathcal{F}_\lambda^h$, $\mathcal{F}_{\lambda+Lh^\alpha}$, $S_{\lambda,h}$, and $\mathcal{K}_{\lambda,h}$. The region $\mathcal{F}_{\lambda+Lh^\alpha}$ is shown in red, while $\mathcal{F}_\lambda^h$ is depicted in grey. The part of $\mathcal{F}_\lambda^h$ not included in $\mathcal{F}_{\lambda+Lh^\alpha}$ corresponds to $S_{\lambda,h}$. The blue region represents the union of segments added to $\mathcal{F}_\lambda^h$ to form $\mathcal{K}_{\lambda,h}$.

where $(.)_+ = \max(.,0)$ denotes the positive part. For $x \in \bigcup_{z \in S_{\lambda,h}} [z, \xi(z)]$, the function $F_{\lambda,h}$ pushes x along the segment

$$\left[x, \xi(x) + (2h - d_2\left(\xi(x), M_i \cap \mathcal{F}_{\lambda+Lh^\alpha}\right))_+ \frac{x - \xi(x)}{||x - \xi(x)||_2}\right] \subset [x, \xi(x)].$$

From a geometric point of view, $F_{\lambda,h}(x)$ pushes in the direction of the normalized vector $-\frac{x-\xi(x)}{||x-\xi(x)||_2}$, which corresponds to the opposite of the gradient of the distance function to the set $\bigcup_{i=1}^l \partial M_i \cap (0,1)^d$ at the point x. This perspective links naturally to existing results that use the (generalized) gradient of the distance function to construct deformation retracts (see for instance Kim et al., 2020, Theorem 12). Moreover, as $\bigcup_{i=1}^l \partial M_i \cap (0,1)^d$ is an $C^{1,1}$ hypersurface, it is worth noting that the vector $-\frac{x-\xi(x)}{||x-\xi(x)||_2}$ generates the normal cone of the hypersurface at $\xi(x)$ (see Federer, 1959, Theorem 4.8.).

Note that the term $(2h - d_2\left(\xi(x), M_i \cap \mathcal{F}_{\lambda+Lh^\alpha}\right))_+$ and the condition (**C1**) will be instrumental in establishing the continuity of $F_{\lambda,h}$, as they ensure that, for any point $x \in \bigcup_{x \in S_{\lambda,h}} [x, \xi(x)] \cap M_i$, the closer x is to $\mathcal{F}_{\lambda+Lh^\alpha} \cap M_i$, the less it will be displaced by the deformation $F_{\lambda,h}$.

Finally, we define

$$\mathcal{G}_{\lambda,h} = \mathrm{Im}\left(x \longmapsto F_{\lambda,h}(x,1)\right),$$

which will serve as our deformation retract. With this, we have all the necessary formalism to state Lemma 2.
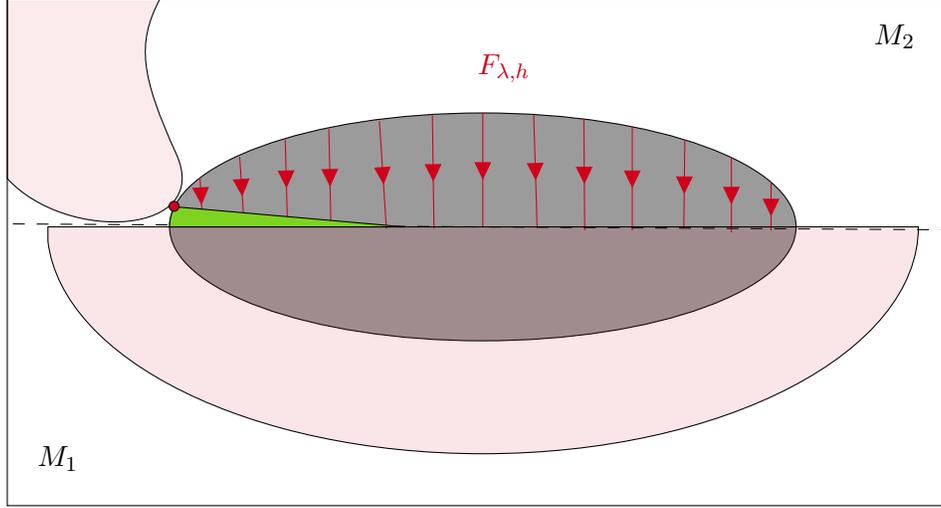
Figure 6: Illustration of the deformation retraction $F_{\lambda,h}$. The region $\mathcal{F}_{\lambda+Lh^\alpha}$ is shown in red, while $\mathcal{F}_\lambda^h$ is depicted in gray. Points closer to $\mathcal{F}_{\lambda+Lh^\alpha}$ experience less displacement under $F_{\lambda,h}$, which ensures its continuity. The green region represents elements of $\mathcal{G}_{\lambda,h}$ that do not belong to $\mathcal{F}_{\lambda+Lh^\alpha}$ but will be included in $\mathcal{F}_{\lambda+\varepsilon}$ for some $\varepsilon \asymp h^\alpha$, as ensured by Assumptions **A1** and **A2** (see proof of Lemma 2).

Lemma 2 *For all $0 < h < \frac{R}{2}$ and $\lambda \in \mathbb{R}$, $F_{\lambda,h}$ is a deformation retraction of $\mathcal{K}_{\lambda,h}$ onto $\mathcal{G}_{\lambda,h}$. Furthermore, we have $\mathcal{F}_\lambda^h \subset \mathcal{K}_{\lambda,h} \subset \mathcal{F}_\lambda^{2h}$ and $\mathcal{F}_\lambda \subset \mathcal{G}_{\lambda,h} \subset \mathcal{F}_{\lambda+L(1+3^\alpha)h^\alpha}$.*

The proof of Lemma 2 is provided in Appendix B.2. Combining the inclusion $\mathcal{F}_\lambda^{\sqrt{dh}} \subset \mathcal{K}_{\lambda,\sqrt{dh}}$, the retraction from $\mathcal{K}_{\lambda,\sqrt{dh}}$ to $\mathcal{G}_{\lambda,\sqrt{dh}}$, and the inclusion $\mathcal{G}_{\lambda,\sqrt{dh}} \subset \mathcal{F}_{\lambda+L(1+3^\alpha)d^{\alpha/2}h^\alpha}$, provided by Lemma 2, induces a morphism from $(H_s(\mathcal{F})_\lambda^{\sqrt{dh}}))_{\lambda\in\mathbb{R}}$ to $\mathbb{V}_{f,s}$.

Now, we construct the morphism from $\mathbb{V}_{f,s}$ to $(H_s(\mathcal{F}_\lambda^{-h}))_{\lambda\in\mathbb{R}}$. The idea is similar to the construction of the previous morphism, with the key difference being that here we want to map points of $\mathcal{F}_\lambda$, that are not in $\mathcal{F}_{\lambda+\varepsilon}^{-h}$ for reasonable ε, into $\mathcal{F}_{\lambda+\varepsilon}^{-h}$. These problematic points are typically contained in:

$$P_{\lambda,h} = \left(\left(\bigcup_{i=1}^l \partial M_i \cap]0,1[^d \right)^h \setminus \mathcal{F}_{\lambda+2Lh^\alpha}^{-h} \right) \cap \mathcal{F}_\lambda,$$

which are located near the boundaries of the regular pieces. The idea is to push these points away from the boundaries. To do this, we define the map:

$$\gamma_h(x) = \begin{cases} x + \frac{\left(h-d_2\left(x,\bigcup_{i=1}^l \partial M_i \cap]0,1[^d\right)\right)}{d_2\left(x,\bigcup_{i=1}^l \partial M_i \cap]0,1[^d\right)} (x-\xi(x)), & \text{if } x \in \left(\bigcup_{i=1}^l \partial M_i \cap]0,1[^d\right)^h \setminus \bigcup_{i=1}^l \partial M_i, \\ x, & \text{if } x \notin \left(\bigcup_{i=1}^l \partial M_i \cap]0,1[^d\right)^h. \end{cases}$$

The function γ_h pushes points from the h-neighborhood of the boundaries by following the gradient of the distance function to $\bigcup_{i=1}^l \partial M_i \cap]0,1[^d$, moving them outside of this h-neighborhood. It should be noted that, for all $x \in \left(\bigcup_{i=1}^l \partial M_i \cap]0,1[^d\right)^h \setminus \bigcup_{i=1}^l \partial M_i$, the

vectors $\gamma_h(x) - x$ and $\xi(x) - x$ are collinear and point in opposite directions. Consequently, $\gamma_h(x) - x$ also generates the normal cone of $\bigcup_{i=1}^{l} \partial M_i \cap]0, 1[^d$ at $\xi(x)$. Moreover, this function can be continuously extended to $P_{\lambda,h}$ using Assumption **A3** (see the proof of Lemma 3). We denote this extension by $\gamma_{h,\lambda}$.
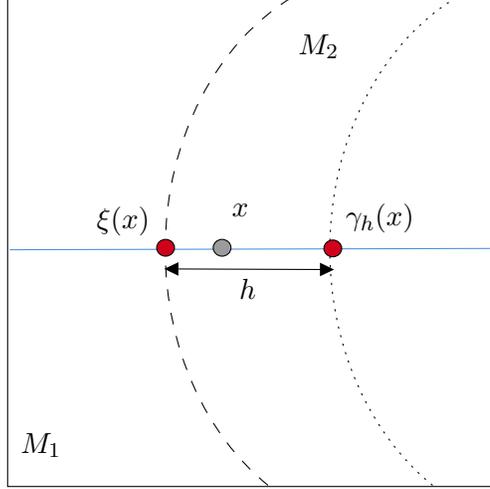

Figure 7: Illustration of ξ and γ_h. In blue is represented the normal cone of $\bigcup_{i=1}^{l} \partial M_i \cap]0, 1[^d$ at $\xi(x)$.

Our goal now is to use $\gamma_{h,\lambda}$ to push smoothly points of $P_{\lambda,h}$, constructing again a deformation retraction. Similarly to what we did in Lemma 2, for some $x \in P_{\lambda,h}$, the line segment $[x, \gamma_{h,\lambda}(x)]$ may not be contained entirely in $\mathcal{F}_\lambda$. Therefore, we consider the larger set, adding the segments $[x, \gamma_{h,\lambda}(x)]$ for all $x \in P_{\lambda,h}$:

$$\mathcal{N}_{\lambda,h} := \mathcal{F}_\lambda \cup \left(\bigcup_{x \in P_{\lambda,h}} [x, \gamma_{h,\lambda}(x)] \right) \subset \mathcal{F}_{\lambda + Lh^\alpha}.$$

To ensure the continuity of the deformation retraction, we need to control how much we move the points of $\bigcup_{x \in P_{\lambda,h}} [x, \gamma_{h,\lambda}(x)] \cap M_i$ that are close to $\mathcal{F}_{\lambda + 2Lh^\alpha} \cap (\overline{M_i})^c$. Thus, we introduce condition (**C2**): there exists $i \in \{1, \dots, l\}$ such that

$$x \in \bigcup_{x \in P_{\lambda,h}} [x, \gamma_{h,\lambda}(x)] \cap M_i \tag{4}$$

and

$$d_2 \left(\gamma_{h,\lambda}(x), (\overline{M_i})^c \cap \mathcal{F}_{\lambda + 2Lh^\alpha} \right) \geq 3h - \|x - \gamma_{h,\lambda}(x)\|_2. \tag{5}$$

We then define $H_{\lambda,h} : \mathcal{N}_{\lambda,h} \times [0,1] \to \mathcal{N}_{\lambda,h}$, which will serve as our deformation retraction, by $H_{\lambda,h}(x) =$

$$\begin{cases} (1-t)x + t \left(\gamma_{h,\lambda}(x) + \left(3h - d_2 \left(\gamma_{h,\lambda}(x), (\overline{M_i})^c \cap \mathcal{F}_{\lambda + 2Lh^\alpha} \right) \right)_+ \frac{x - \gamma_{h,\lambda}(x)}{\|x - \gamma_{h,\lambda}(x)\|_2} \right), & \text{if (\textbf{C2})}, \\ x, & \text{else.} \end{cases}$$
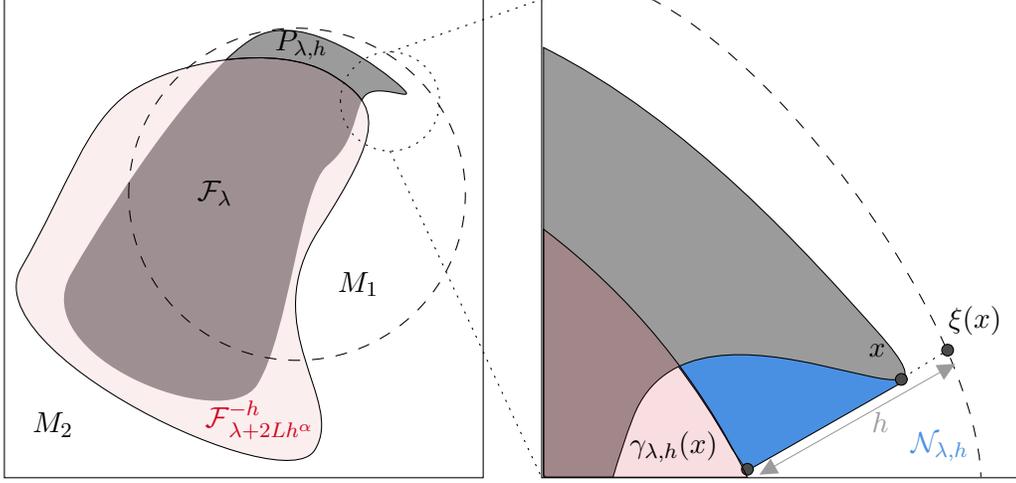
Figure 8: Illustration of the sets $\mathcal{F}_\lambda$, $\mathcal{F}_{\lambda+2Lh^\alpha}^{-h}$, $P_{\lambda,h}$, and $\mathcal{N}_{\lambda,h}$. The region $\mathcal{F}_{\lambda+2Lh^\alpha}^{-h}$ is shown in red, while $\mathcal{F}_\lambda$ is depicted in gray. The part of $\mathcal{F}_\lambda$ not included in $\mathcal{F}_{\lambda+2Lh^\alpha}^{-h}$ corresponds to $P_{\lambda,h}$. The blue region represents the union of segments added to $\mathcal{F}_\lambda$ to form $\mathcal{N}_{\lambda,h}$.

Finally, we denote $\mathcal{M}_{\lambda,h} = \mathrm{Im}(x \mapsto H_{\lambda,h}(x,1))$, which will serve as our deformation retract. We can now state Lemma 3.
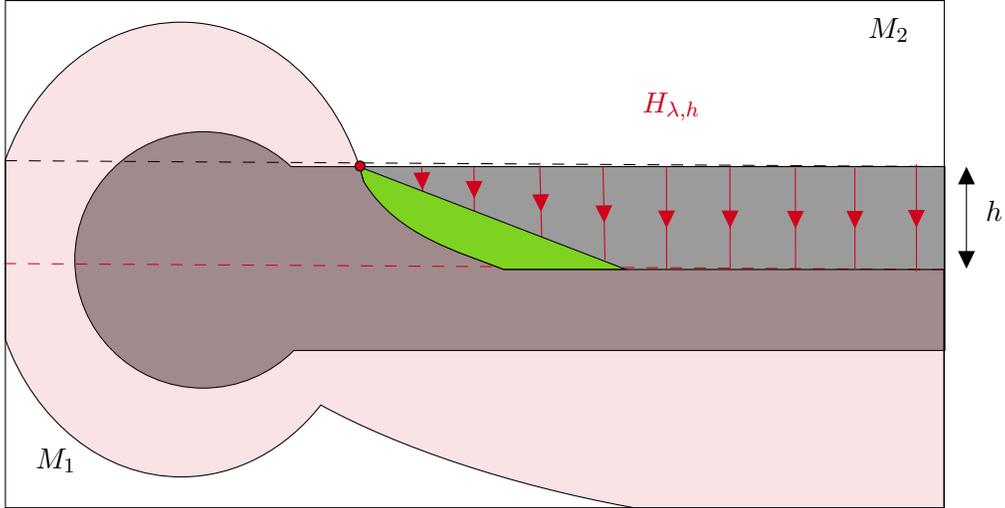
Figure 9: Illustration of the deformation retraction $H_{\lambda,h}$. The region $\mathcal{F}_{\lambda+2Lh^\alpha}^{-h}$ is shown in red, while $\mathcal{F}_\lambda$ is depicted in gray. Points closer to $\mathcal{F}_{\lambda+2Lh^\alpha}^{-h}$ experience less displacement under $F_{\lambda,h}$, which ensures its continuity. The green region represents elements of $\mathcal{M}_{\lambda,h}$ that do not belong to $\mathcal{F}_{\lambda+2Lh^\alpha}^{-h}$ but will be included in $\mathcal{F}_{\lambda+\varepsilon}^{-h}$ for some $\varepsilon \asymp h^\alpha$ (see proof of Lemma 3).

Lemma 3 *For all $0 < h < \frac{R}{2}$ and $\lambda \in \mathbb{R}$, $H_{\lambda,h}$ is a deformation retraction from $\mathcal{N}_{\lambda,h}$ onto $\mathcal{M}_{\lambda,h}$. Furthermore, we have $\mathcal{F}_\lambda^{-h} \subset \mathcal{M}_{\lambda,h} \subset \mathcal{F}_{\lambda+(2+5\alpha)Lh^\alpha}^{-h}$ and $\mathcal{F}_\lambda \subset \mathcal{N}_{\lambda,h} \subset \mathcal{F}_{\lambda+Lh^\alpha}$.*

The proof of Lemma 3 is provided in Appendix B.4. Similarly to Lemma 2, Lemma 3 provides a morphism from $\mathbb{V}_{f,s}$ to $(H_s(\mathcal{F}_\lambda^{-\sqrt{d}h}))_{\lambda \in \mathbb{R}}$.

Next, we state a technical result: Lemma 4, which will allow us to prove that the morphisms we constructed previously induce an interleaving.

Lemma 4 *Let $\lambda \in \mathbb{R}$ and $h \asymp \left(\frac{\log(n)}{n}\right)^{\frac{1}{d+2\alpha}}$, for sufficiently large n, we have, for all $f \in S_d(M, L, \alpha, R)$, for all $x \in \widehat{\mathcal{F}}_\lambda \cap S_{\lambda + \sqrt{2}\sigma N_h h^\alpha, \sqrt{d}h}$,*

$$[x, \xi(x)] \subset \widehat{\mathcal{F}}_{\lambda + (c_1\sqrt{2}\sigma N_h + c_2)h^\alpha} \tag{6}$$

and for all $x \in \widehat{\mathcal{F}}_\lambda \cap P_{\lambda, \sqrt{d}h}$,

$$\left[x, \gamma_{\lambda, \sqrt{d}h}(x)\right] \subset \widehat{\mathcal{F}}_{\lambda + (c_1\sqrt{2}\sigma N_h + c_2)h^\alpha} \tag{7}$$

with $c_1 = 2(1 + (2d)^d)$, $c_2 = (1 + (2d)^d)(5L\sqrt{d} + 2\kappa M)$ and κ a constant depending only on d and R.

In particular, as $\widehat{\mathcal{F}}_\lambda \subset \mathcal{F}_{\lambda + \sqrt{2}\sigma N_h h^\alpha}^{\sqrt{d}h}$ (by Lemma 1), Assertion (6) of Lemma 4 ensures that, for sufficiently large n and for all $x \in \widehat{\mathcal{F}}_\lambda$:

$$F_{\lambda + \sqrt{2}\sigma N_h h^\alpha, \sqrt{d}h}(x, [0,1]) \subset \widehat{\mathcal{F}}_{\lambda + ch}$$

for some constant c depending on the model parameters and N_h. This implies that any chain $C \in C_s(\widehat{\mathcal{F}}_\lambda)$, $s \in \mathbb{N}$, is homologically equivalent, within $\widehat{\mathcal{F}}_{\lambda + ch}$, to its deformed counterpart:

$$F_{\lambda + \sqrt{2}\sigma N_h h^\alpha, \sqrt{d}h}^{\#}(C, 1).$$

Similar guarantees also hold for the deformation retraction involved in Lemma 3. More precisely, it follows from Assertion (7) of Lemma 4, that for all $x \in \widehat{\mathcal{F}}_\lambda \cap \mathcal{F}_\lambda$,

$$H_{\lambda, \sqrt{d}h}(x, [0,1]) \subset \widehat{\mathcal{F}}_{\lambda + ch}$$

and consequently for any $C \in C_s\left(\widehat{\mathcal{F}}_\lambda \cap \mathcal{F}_\lambda\right)$, C is homologically equivalent, within $\widehat{\mathcal{F}}_{\lambda + ch}$ to:

$$H_{\lambda, \sqrt{d}h}^{\#}(C, 1).$$

These key properties will be instrumental in showing that the morphisms ϕ and ψ satisfy Definition 9, in particular, to prove that the diagrams involved commute. This will allow us to establish an interleaving with a constant depending on N_h. To complete the proof, we will therefore require a concentration inequality for N_h, which is stated in the following lemma and proved in Appendix B.7.

Lemma 5 *Let $h > \frac{1}{N}$,*

$$\mathbb{P}\left(N_h \geq t\right) \leq 2\left(\frac{1}{h}\right)^d \exp\left(-t^2 \log\left(1/h^d\right)\right).$$

Consequently, there exist two constants C_0 and C_1 depending only on d such that, for all $h < 1$,

$$\mathbb{P}\left(N_h \leq t\right) \leq C_0 \exp\left(-C_1 t^2\right).$$

Equipped with these lemmas, we can now prove Theorem 1, from which follows Theorem 2.

Theorem 1 *Let $h \asymp \left(\frac{\log(n)}{n}\right)^{\frac{1}{d+2\alpha}}$. There exist $\tilde{C}_0$ and $\tilde{C}_1$ (depending only on M, L, α, R and σ) such that, for all $t > 0$,*

$$\sup_{f \in S_d(M,L,\alpha,R)} \mathbb{P}\left(d_b\left(\widehat{\mathrm{dgm}(f)}, \mathrm{dgm}(f)\right) \geq t\left(\frac{\log(n)}{n}\right)^{\frac{\alpha}{d+2\alpha}}\right) \leq \tilde{C}_0 \exp\left(-\tilde{C}_1 t^2\right).$$

Proof It suffices to show the result for large n (up to rescaling $\tilde{C}_0$). Hence, we assume that n is such that $2\sqrt{dh} < R$ and Lemma 4 holds. The proof is essentially a combination of the lemmas stated throughout this section. We begin by specifying the exact construction of ϕ_λ, which will be obtained by the composition of the following linear maps:

$$j_{1,\lambda} : H_s\left(\widehat{\mathcal{F}}_\lambda\right) \to H_s\left(\mathcal{K}_{\lambda+\sqrt{2}\sigma N_h h^\alpha, \sqrt{dh}}\right)$$

the map induced by the inclusion $\widehat{\mathcal{F}}_\lambda \subset \mathcal{F}^{\sqrt{dh}}_{\lambda+\sqrt{2}\sigma N_h h^\alpha} \subset \mathcal{K}_{\lambda+\sqrt{2}\sigma N_h h^\alpha, \sqrt{dh}}$ obtained by combining Lemma 1 and 2,

$$j_{2,\lambda} : H_s\left(\mathcal{K}_{\lambda+\sqrt{2}\sigma N_h h^\alpha, \sqrt{dh}}\right) \to H_s\left(\mathcal{G}_{\lambda+\sqrt{2}\sigma N_h h^\alpha, \sqrt{dh}}\right)$$

induced by the deformation retraction from Lemma 2, and, with $k_1 = Ld^{\alpha/2}\left(1 + 3^\alpha\right) + c_2$,

$$j_{3,\lambda} : H_s\left(\mathcal{G}_{\lambda+\sqrt{2}\sigma N_h h^\alpha, \sqrt{dh}}\right) \to H_s\left(\mathcal{F}_{\lambda+\left(k_1+(1+c_1)\sqrt{2}\sigma N_h\right)h^\alpha}\right)$$

the map induced by inclusion, following again from Lemma 2. Now, we can define:

$$\begin{cases} \phi_\lambda : H_s\left(\widehat{\mathcal{F}}_\lambda\right) \to H_s\left(\mathcal{F}_{\lambda+\left(k_1+(1+c_1)\sqrt{2}\sigma N_h\right)h^\alpha}\right) \\ \phi_\lambda = j_{3,\lambda} \circ j_{2,\lambda} \circ j_{1,\lambda} \end{cases}$$

This provides the first persistence module morphism ϕ. Let us construct the second one by specifying the construction of ψ_λ, which will be obtained by composition of the following linear maps:

$$j_{4,\lambda} : H_s\left(\mathcal{F}_\lambda\right) \to H_s\left(\mathcal{N}_{\lambda, \sqrt{dh}}\right)$$

the map induced by the inclusion $\mathcal{F}_\lambda \subset \mathcal{N}_{\lambda, \sqrt{dh}}$ from Lemma 3,

$$j_{5,\lambda} : H_s\left(\mathcal{N}_{\lambda, \sqrt{dh}}\right) \to H_s\left(\mathcal{M}_{\lambda, \sqrt{dh}}\right)$$

the map induced by the deformation retraction from Lemma 3, and, with $k_2 = Ld^{\alpha/2}(2 + 5^\alpha) + c_2$,

$$j_{6,\lambda} : H_s\left(\mathcal{M}_{\lambda, \sqrt{dh}}\right) \to H_s\left(\widehat{\mathcal{F}}_{\lambda+\left(k_2+(1+c_1)\sqrt{2}\sigma N_h\right)h^\alpha}\right)$$

induced by the inclusion $\mathcal{M}_{\lambda, \sqrt{dh}} \subset \mathcal{F}^{-\sqrt{dh}}_{\lambda+k_2 h^\alpha} \subset \widehat{\mathcal{F}}_{\lambda+\left(k_2+(1+c_1)\sqrt{2}\sigma N_h\right)h^\alpha}$, from the combination of Lemma 1 and 3. We then define:

$$\begin{cases} \psi_\lambda : H_s\left(\mathcal{F}_\lambda\right) \longrightarrow H_s\left(\widehat{\mathcal{F}}_{\lambda+\left(k_2+(1+c_1)\sqrt{2}\sigma N_h\right)h^\alpha}\right) \\ \psi_\lambda = j_{6,\lambda} \circ j_{5,\lambda} \circ j_{4,\lambda} \end{cases}$$

20

which provides the second morphism ψ. Now, we show that ψ and ϕ induce an interleaving between $\widehat{\mathbb{V}}_{f,s}$ and $\mathbb{V}_{s,f}$. More precisely, we show that the following diagrams commute for all $\lambda < \lambda'$. For compactness of notations, let $K_1 = k_1 + (1 + c_1)\sqrt{2}\sigma N_h$ and $K_2 = k_2 + (1 + c_1)\sqrt{2}\sigma N_h$.

$$
\begin{array}{ccc}
H_s\left(\widehat{\mathcal{F}}_\lambda\right) & \xrightarrow{\widehat{v}_\lambda^{\lambda'}} & H_s\left(\widehat{\mathcal{F}}_{\lambda'}\right) \\
\downarrow{\scriptstyle\phi_\lambda} & & \downarrow{\scriptstyle\phi_{\lambda'}} \\
H_s\left(\mathcal{F}_{\lambda+K_1h^\alpha}\right) & \xrightarrow{v_{\lambda+K_1h^\alpha}^{\lambda'+K_1h^\alpha}} & H_s\left(\mathcal{F}_{\lambda'+K_1h^\alpha}\right)
\end{array}
\tag{8}
$$

$$
\begin{array}{ccc}
H_s\left(\mathcal{F}_\lambda\right) & \xrightarrow{v_\lambda^{\lambda'}} & H_s\left(\mathcal{F}_{\lambda'}\right) \\
\downarrow{\scriptstyle\psi_\lambda} & & \downarrow{\scriptstyle\psi_{\lambda'}} \\
H_s\left(\widehat{\mathcal{F}}_{\lambda+K_2h^\alpha}\right) & \xrightarrow{\widehat{v}_{\lambda+K_2h^\alpha}^{\lambda'+K_2h^\alpha}} & H_s\left(\widehat{\mathcal{F}}_{\lambda'+K_2h^\alpha}\right)
\end{array}
\tag{9}
$$

$$
\begin{array}{ccc}
H_s\left(\widehat{\mathcal{F}}_\lambda\right) & \xrightarrow{\widehat{v}_\lambda^{\lambda+(K_1+K_2)h^\alpha}} & H_s\left(\widehat{\mathcal{F}}_{\lambda+(K_1+K_2)h^\alpha}\right) \\
& {\scriptstyle\phi_\lambda}\searrow \quad {\scriptstyle\psi_{\lambda+K_1h^\alpha}}\nearrow & \\
& H_s\left(\mathcal{F}_{\lambda+K_1h^\alpha}\right) &
\end{array}
\tag{10}
$$

$$
\begin{array}{ccc}
H_s\left(\mathcal{F}_\lambda\right) & \xrightarrow{v_\lambda^{\lambda+(K_1+K_2)h^\alpha}} & H_s\left(\mathcal{F}_{\lambda+(K_1+K_2)h^\alpha}\right) \\
& {\scriptstyle\psi_\lambda}\searrow \quad {\scriptstyle\phi_{\lambda+K_2h^\alpha}}\nearrow & \\
& H_s\left(\widehat{\mathcal{F}}_{\lambda+K_2h^\alpha}\right) &
\end{array}
\tag{11}
$$

21

- **Diagram 8:** We can rewrite the diagram as (unspecified maps are simply induced by set inclusion),

$$
\begin{array}{ccc}
H_s\left(\widehat{\mathcal{F}}_\lambda\right) & \xrightarrow{\;\widehat{v}_\lambda^{\lambda'}\;} & H_s\left(\widehat{\mathcal{F}}_{\lambda'}\right) \\
\downarrow & & \downarrow \\
H_s\left(\mathcal{K}_{\lambda+\sqrt{2}\sigma N_h h^\alpha,\sqrt{dh}}\right) & \longrightarrow & H_s\left(\mathcal{K}_{\lambda'+\sqrt{2}\sigma N_h h^\alpha,\sqrt{dh}}\right) \\
\updownarrow{\scriptstyle j_{2,\lambda}} & & \updownarrow{\scriptstyle j_{2,\lambda'}} \\
H_s\left(\mathcal{G}_{\lambda+\sqrt{2}\sigma N_h h^\alpha,\sqrt{dh}}\right) & \longrightarrow & H_s\left(\mathcal{G}_{\lambda'+\sqrt{2}\sigma N_h h^\alpha,\sqrt{dh}}\right) \\
\downarrow & & \downarrow \\
H_s\left(\mathcal{F}_{\lambda+K_1 h^\alpha}\right) & \xrightarrow{\;\widehat{v}_{\lambda+K_1 h^\alpha}^{\lambda'+K_1 h^\alpha}\;} & H_s\left(\mathcal{F}_{\lambda'+K_1 h^\alpha}\right)
\end{array}
$$

As $j_{2,\lambda}$ and $j_{2,\lambda'}$ arise from deformation retractions and other maps are simply induced by inclusion, all faces of Diagram 8 commute. Consequently, Diagram 8 commutes.

- **Diagram 9:** it can be decomposed similarly to Diagram 8. One can check that the same reasoning applies.

- **Diagram 10:** Here, the proof is slightly more technical and requires more subtle geometric arguments, in particular involving Lemma 4. Let $C \in C_s\left(\widehat{\mathcal{F}}_\lambda\right)$ and $[C]$ be its classes in $H_s\left(\widehat{\mathcal{F}}_\lambda\right)$. To prove the commutativity of Diagram 10, it suffices to show that:

$$
\psi_{\lambda+K_1 h_\alpha}\left(\phi_\lambda([C])\right) = [C] \in H_s\left(\widehat{\mathcal{F}}_{\lambda+(K_1+K_2)h^\alpha}\right). \tag{12}
$$

First, observe that ϕ_λ maps $[C]$ to $[C']$ with,

$$
C' = F^{\#}_{\lambda+\sqrt{2}\sigma N_h h^\alpha,\sqrt{dh}}(C,1).
$$

We begin by proving that:

$$
[C'] = [C] \in H_s\left(\widehat{\mathcal{F}}_{\lambda+(K_1+K_2)h^\alpha}\right). \tag{13}
$$

Denote $\overline{F}_{\lambda+\sqrt{2}\sigma N_h h^\alpha,\sqrt{dh}}$ the restriction of $F_{\lambda+\sqrt{2}\sigma N_h h^\alpha,\sqrt{dh}}$ to:

$$
F_{\lambda+\sqrt{2}\sigma N_h h^\alpha,\sqrt{dh}}(\widehat{\mathcal{F}}_\lambda,[0,1]).
$$

It is a deformation retraction from

$$
F_{\lambda+\sqrt{2}\sigma N_h h^\alpha,\sqrt{dh}}(\widehat{\mathcal{F}}_\lambda,[0,1])
$$

to

$$
F_{\lambda+\sqrt{2}\sigma N_h h^\alpha,\sqrt{dh}}(\widehat{\mathcal{F}}_\lambda,1).
$$

22

Thus, by homology invariance under deformation retraction,

$$
\begin{aligned}
[C] &= \left[\overline{F}^{\#}_{\lambda + \sqrt{2}\sigma N_h h^\alpha, \sqrt{d}h}(C, 1) \right] \\
&= \left[F^{\#}_{\lambda + \sqrt{2}\sigma N_h h^\alpha, \sqrt{d}h}(C, 1) \right] \\
&= [C'] \in H_s \left(F_{\lambda + \sqrt{2}\sigma N_h h^\alpha, \sqrt{d}h}(\widehat{\mathcal{F}}_\lambda, [0, 1]) \right).
\end{aligned}
$$

Assertion (6) of Lemma 4 ensures that

$$
F_{\lambda + \sqrt{2}\sigma N_h h^\alpha, \sqrt{d}h}(\widehat{\mathcal{F}}_\lambda, [0, 1]) \subset \widehat{\mathcal{F}}_{\lambda + K_1 h^\alpha}
$$

and thus,

$$
[C] = [C'] \in H_s \left(\widehat{\mathcal{F}}_{\lambda + K_1 h^\alpha} \right).
$$

As $\widehat{\mathcal{F}}_{\lambda + K_1 h^\alpha} \subset \widehat{\mathcal{F}}_{\lambda + (K_1 + K_2) h^\alpha}$, this proves (13). Next, as $C' \in C_s(\widehat{\mathcal{F}}_{\lambda + K_1 h^\alpha} \cap \mathcal{F}_{\lambda + K_1 h^\alpha})$, $\psi_{\lambda + K_1 h^\alpha}$ maps $[C']$ to $[C'']$, with,

$$
C'' = H^{\#}_{\lambda + K_1 h^\alpha, \sqrt{d}h}(C', 1).
$$

Let us prove that:

$$
[C'] = [C''] \in H_s \left(\widehat{\mathcal{F}}_{\lambda + (K_1 + K_2) h^\alpha} \right). \tag{14}
$$

Denote $\overline{H}_{\lambda + K_1 h^\alpha, \sqrt{d}h}$ the restriction of $H_{\lambda + K_1 h^\alpha, \sqrt{d}h}$ to:

$$
H_{\lambda + K_1 h^\alpha, \sqrt{d}h} \left(\widehat{\mathcal{F}}_{\lambda + K_1 h^\alpha} \cap \mathcal{F}_{\lambda + K_1 h^\alpha}, [0, 1] \right).
$$

It is a deformation retraction and thus, again, by homology invariance under deformation retract,

$$
\begin{aligned}
[C'] &= \left[\overline{H}^{\#}_{\lambda + K_1 h^\alpha, \sqrt{d}h}(C', 1) \right] \\
&= \left[H^{\#}_{\lambda + K_1 h^\alpha, \sqrt{d}h}(C', 1) \right] \\
&= [C''] \in H_s \left(H_{\lambda + K_1 h^\alpha, \sqrt{d}h} \left(\widehat{\mathcal{F}}_{\lambda + K_1 h^\alpha} \cap \mathcal{F}_{\lambda + K_1 h^\alpha}, [0, 1] \right) \right)
\end{aligned}
$$

Assertion (7) of Lemma 4 then ensures that:

$$
H_{\lambda + K_1 h^\alpha, \sqrt{d}h} \left(\widehat{\mathcal{F}}_{\lambda + K_1 h^\alpha} \cap \mathcal{F}_{\lambda + K_1 h^\alpha}, [0, 1] \right) \subset \widehat{\mathcal{F}}_{\lambda + (K_1 + K_2) h^\alpha}
$$

and consequently proves (14). Combining (14) and (13) we have (12) and therefore Diagram 10 commutes.

- **Diagram 11:** Let $C \in C_s(\mathcal{F}_\lambda)$, ψ_λ maps $[C]$ to $[C']$, with,

$$
C' = H^{\#}_{\lambda, \sqrt{d}h}(C, 1).
$$

As $\mathcal{M}_{\lambda,\sqrt{d}h} \subset \mathcal{G}_{\lambda+K_2 h^\alpha, \sqrt{d}h}$, the linear map $\phi_{\lambda+K_2 h^\alpha}$ behaves as an inclusion induced map, mapping $[C']$ to $[C']$. From Lemma 3, we have:

$$H_{\lambda,\sqrt{d}h}(\mathcal{F}_\lambda, [0,1]) \subset \mathcal{N}_{\lambda,\sqrt{d}h} \subset \mathcal{F}_{\lambda+(K_1+K_2)h^\alpha}.$$

Thus,

$$[C] = [C'] \in H_s\left(\mathcal{F}_{\lambda+(K_1+K_2)h^\alpha}\right)$$

and Diagram 11 commutes.

The commutativity of diagrams 9,8,10 and 11 means that $\widehat{\mathbb{V}}_{f,s}$ and $\mathbb{V}_{f,s}$ are $(K_1+K_2)h^\alpha$ interleaved, and thus we get from the algebraic stability theorem (Chazal et al., 2009) that

$$d_b\left(\mathrm{dgm}\left(\widehat{\mathbb{V}}_{f,s}\right), \mathrm{dgm}\left(\mathbb{V}_{f,s}\right)\right) \le (K_1+K_2)h^\alpha$$

and as it holds for all $s \in \mathbb{N}$,

$$d_b\left(\widehat{\mathrm{dgm}(f)}, \mathrm{dgm}(f)\right) \le (K_1+K_2)h^\alpha.$$

Now, using Lemma 5, this implies that, for all $f \in S_d(M,L,\alpha,R)$,

$$\mathbb{P}\left(d_b\left(\widehat{\mathrm{dgm}(f)}, \mathrm{dgm}(f)\right) \ge th^\alpha\right)$$

$$\le \mathbb{P}\left(K_1+K_2 \ge t\right)$$

$$= \mathbb{P}\left(N_h \ge \frac{t-k_1-k_2}{2\sqrt{2}\sigma(1+c_1)}\right)$$

$$\le C_0 \exp\left(-C_1\left(\frac{t-k_1-k_2}{2\sqrt{2}\sigma(1+c_1)}\right)^2\right)$$

$$\le C_0 \exp\left(2\frac{C_1(k_1+k_2)}{\left(2\sqrt{2}\sigma(1+c_1)\right)^2}t\right)\exp\left(-C_1\left(\frac{k_1+k_2}{2\sqrt{2}\sigma(1+c_1)}\right)^2\right)$$

$$\times \exp\left(-\frac{C_1}{\left(2\sqrt{2}\sigma(1+c_1)\right)^2}t^2\right)$$

$$= C_0 \exp\left(-C_1\left(\frac{k_1+k_2}{\left(2\sqrt{2}\sigma(1+c_1)\right)}\right)^2\right)\exp\left(2\frac{C_1(k_1+k_2)}{\left(2\sqrt{2}\sigma(1+c_1)\right)^2}t - \frac{C_1}{2\left(2\sqrt{2}\sigma(1+c_1)\right)^2}t^2\right)$$

$$\times \exp\left(-\frac{C_1}{2\left(2\sqrt{2}\sigma(1+c_1)\right)^2}t^2\right)$$

Now, as for all $t \in \mathbb{R}$,

$$2\frac{C_1(k_1+k_2)}{\left(2\sqrt{2}\sigma(1+c_1)\right)^2}t - \frac{C_1}{2\left(2\sqrt{2}\sigma(1+c_1)\right)^2}t^2 \le \frac{2C_1(k_1+k_2)^2}{\left(2\sqrt{2}\sigma(1+c_1)\right)^2}$$

we have:

$$\mathbb{P}\left(d_b\left(\widehat{\mathrm{dgm}(f)}, \mathrm{dgm}(f)\right) \ge th^\alpha\right)$$

$$\leq C_0 \exp\left(-C_1 \left(\frac{k_1 + k_2}{(2\sqrt{2}\sigma(1 + c_1))}\right)^2 + \frac{2C_1(k_1 + k_2)^2}{(2\sqrt{2}\sigma(1 + c_1))^2}\right) \exp\left(-\frac{C_1}{2\left(2\sqrt{2}\sigma(1 + c_1)\right)^2}t^2\right)$$

$$= C_0 \exp\left(\frac{C_1(k_1 + k_2)^2}{\left(2\sqrt{2}\sigma(1 + c_1)\right)^2}\right) \exp\left(-\frac{C_1}{2\left(2\sqrt{2}\sigma(1 + c_1)\right)^2}t^2\right)$$

and the result follows. ∎

We can derive from this result bounds in expectation, proving Theorem 2.

Theorem 2 *Let* $h \asymp \left(\frac{\log(n)}{n}\right)^{\frac{1}{d+2\alpha}}$,

$$\sup_{f \in S_d(M, L, \alpha, R)} \mathbb{E}\left(d_b\left(\widehat{\mathrm{dgm}(f)}, \mathrm{dgm}(f)\right)\right) \lesssim \left(\frac{\log(n)}{n}\right)^{\frac{\alpha}{d+2\alpha}}$$

Proof The sub-Gaussian concentration provided by Theorem 1 ensures that, for all $t > 0$,

$$\mathbb{P}\left(\frac{d_b\left(\widehat{\mathrm{dgm}(f)}, \mathrm{dgm}(f)\right)}{h^\alpha} \geq t\right) \leq \tilde{C}_0 \exp\left(-\tilde{C}_1 t^2\right)$$

Now, we have:

$$\mathbb{E}\left(\frac{d_b\left(\widehat{\mathrm{dgm}(f)}, \mathrm{dgm}(f)\right)}{h^\alpha}\right)$$

$$= \int_0^{+\infty} \mathbb{P}\left(\frac{d_b\left(\widehat{\mathrm{dgm}(f)}, \mathrm{dgm}(f)\right)}{h^\alpha} \geq t\right) dt$$

$$\leq \int_0^{+\infty} \tilde{C}_0 \exp\left(-\tilde{C}_1 t^2\right) dt < +\infty.$$

∎

4. Lower Bounds

In this section, we prove that the rates obtained in the previous section are optimal by deriving lower bounds on the minimax risk.

Theorem 3

$$\inf_{\widehat{\mathrm{dgm}(f)}} \sup_{f \in S_d(M, L, \alpha, R)} \mathbb{E}\left(d_b\left(\widehat{\mathrm{dgm}(f)}, \mathrm{dgm}(f)\right)\right) \gtrsim \left(\frac{\log(n)}{n}\right)^{\frac{\alpha}{d+2\alpha}}.$$

Where the infimum is taken over all the estimators of $\mathrm{dgm}(f)$.

The proof follows a standard method to provide minimax lower bounds, as presented in Section 2 of Tsybakov (2008). The idea is, for any $r_n = o\left(\left(\frac{\log(n)}{n}\right)^{\frac{\alpha}{d+2\alpha}}\right)$, to exhibit a finite collection of functions in $S_d(M, L, \alpha, R)$ such that their persistence diagrams are pairwise at distance $2r_n$ but indistinguishable, with high certainty.

Proof Let

$$f_0(x_1, ..., x_d) = \frac{\min(M, L)}{2\sqrt{d}}|x_1|^\alpha$$

and for m integer in $[0, \lfloor 1/h \rfloor]$,

$$f_{h,m}(x_1, ..., x_d) = f_0 - \frac{\min(L, M)}{\sqrt{d}}\left(h^\alpha - ||(x_1, ..., x_d) - m/\lfloor 1/h \rfloor(1, ..., 1)||_\infty^\alpha\right)_+$$

f_0 and the $f_{h,m}$ are $(L, \alpha)-$Hölder-continuous and bounded by M. Thus, they belong to $S_d(M, L, \alpha, R)$ for all $R > 0$.

We have $\text{dgm}(f_0) = \{(0, +\infty)\}$ and for all $0 < m < \lfloor 1/h \rfloor$, integer, $\text{dgm}(f_{h,m}) =$

$$\left\{(0, +\infty), \left(\frac{\min(L, M)}{2\sqrt{d}}\left(\frac{m}{\lfloor 1/h \rfloor}\right)^\alpha - \frac{L}{\sqrt{d}}h^\alpha, \frac{\min(L, M)}{2\sqrt{d}}\left(\frac{m}{\lfloor 1/h \rfloor}\right)^\alpha - \frac{\min(L, M)}{2\sqrt{d}}h^\alpha\right)\right\}.$$

Thus, for all $0 < m \neq m' < \lfloor 1/h \rfloor$, integers,

$$d_b\left(\text{dgm}(f_0), \text{dgm}(f_{m,h})\right) \geq \frac{\min(L, M)h^\alpha}{2\sqrt{d}} \text{ and } d_b\left(\text{dgm}(f_{m,h}), \text{dgm}(f_{m'})\right) \geq \frac{\min(L, M)h^\alpha}{2\sqrt{d}}.$$

We set $r_n = \frac{\min(L,M)h^\alpha}{4\sqrt{d}}$, then,

$$d_b\left(\text{dgm}(f_0), \text{dgm}(f_{d,h,m^{k'},\alpha})\right) \geq 2r_n \text{ and } d_b\left(\text{dgm}(f_{h,m}), \text{dgm}(f_{h,m'})\right) \geq 2r_n.$$

For a fixed signal f, denote $\mathbb{P}_f^n = \bigotimes^n \mathbb{P}_f$ the joint distribution of the observations $X_1, ..., X_n$. From Theorem 2.5 of Tsybakov (2008), it now suffices to show that if $r_n = o\left(\left(\frac{\log(n)}{n}\right)^{\frac{\alpha}{d+2\alpha}}\right)$, then,

$$\frac{1}{\left(\lfloor \frac{1}{h} \rfloor - 2\right)\log\left(\lfloor \frac{1}{h} \rfloor - 2\right)}\sum_{0 < m < \lfloor 1/h \rfloor} KL\left(\mathbb{P}_{f_{h,m}}^n, \mathbb{P}_{f_0}^n\right) \tag{15}$$

converges to zero when n converges to infinity, where KL is the Kullback-Leibler divergence between probability distributions. We denote H_m the hypercube defined by $||(x_1, ..., x_d) - m/\lfloor 1/h \rfloor(1, ..., 1)||_\infty \leq h$

$$KL\left(\mathbb{P}_{f_{h,m}}^n, \mathbb{P}_{f_0}^n\right)$$
$$= \sum_{i=1}^n KL\left(\mathcal{N}(f_{h,m}(x_i), \sigma), \mathcal{N}(f_0(x_i), \sigma)\right)$$
$$= \sum_{i=1}^n \frac{(f_{h,m}(x_i) - f_0(x_i))^2}{2\sigma^2}$$

26

$$= \sum_{x_i \in H_m} \frac{(f_{h,m}(x_i) - f_0(x_i))^2}{2\sigma^2}$$

$$= \frac{\min(M,L)^2}{4d\sigma^2} \sum_{x_i \in H_m} (h^\alpha - ||x_i - m/\lfloor 1/h \rfloor(1,...,1)||_\infty^\alpha)_+^2$$

$$\leq \frac{\min(M,L)^2}{4d\sigma^2} |H_m \cap G_n| h^{2\alpha}$$

$$\lesssim n h^{2\alpha+d}$$

Hence, if $h = o\left(\left(\frac{\log(n)}{n}\right)^{\frac{1}{d+2\alpha}}\right)$, we have that (15) converges to zero. Consequently, if $r_n = o\left(\left(\frac{\log(n)}{n}\right)^{\frac{\alpha}{d+2\alpha}}\right)$, then $h = o\left(\left(\frac{\log(n)}{n}\right)^{\frac{1}{d+2\alpha}}\right)$ and we get the conclusion. ∎

Following the remark made in the Introduction, it is worth noting that the previous proof establishes a stronger result. Throughout the proof, we have only considered (L, α)-Hölder continuous functions, implying that the lower bound we obtain also applies to the minimax risk over Hölder spaces. As a direct consequence, this formally confirms that the rates obtained in Bubenik et al. (2009) and Chung et al. (2009) are minimax.

5. Numerical Illustrations

The present work focuses mainly on addressing the statistical difficulty of estimating persistence diagrams for noisy signals. However, for practical applicability, the computational aspects of the proposed strategy should also be discussed. Although it is easy to implement, it suffers from computational limitations. Since the proposed estimator constructs persistence diagrams using cubical homology, for a window size h, it requires, in the worst case, $O(h^{-d})$ memory to store the cubical complex associated with the sublevel filtration, and the computation of persistence diagrams runs in $O(h^{-3d})$. Following Theorem 1, the h that leads to the minimax convergence rate is of order $O((\ln(n)/n)^{1/(2\alpha+d)})$, which then induces a complexity of $O(n^{d/(2\alpha+d)}) = O(n)$ in memory and $O(n^{3d/(2\alpha+d)}) = O(n^3)$ in computation, which can be prohibitive in many practical scenarios. Note that this is not specific to our method. Any standard plug-in estimator suffers from similar shortcomings. This is likely the main limitation preventing the broader use of persistence diagrams in signal processing. However, efficient computation of persistent homology for cubical complexes is an active area of research (see e.g., Wagner et al., 2012; Jaquette and Kramár, 2015; Otter et al., 2017; Dłotko and Wanner, 2018; Kaji et al., 2020), and the proposed methods may benefit from future progress in this direction. Also note that in some cases, this complexity can be improved. For example, if one is only interested in 0th-order persistent homology (i.e., tracking the evolution of connected components), the complexity for computing the H_0-persistence diagram reduces to $O(h^{-d}\alpha(h^{-d})) = O(n\,\alpha(n))$, where α denotes the inverse of the Ackermann function (see Wagner et al., 2012, Section VII.2). Since α grows extremely slowly, this implies that the algorithm runs essentially in linear time in this case.

Nonetheless, we believe that our strategy can still be valuable in certain practical scenarios, particularly in lower-dimensional settings. To illustrate this, we provide numerical

examples in dimension two, situating ourselves in the common practical scenario of image analysis in the presence of additive noise. In this context, Assumptions **A0**-**A3** essentially allow us to consider images displaying objects with smooth boundaries, with no intersections between objects' boundaries or between objects and the boundary of the image. We consider the following two toy examples:
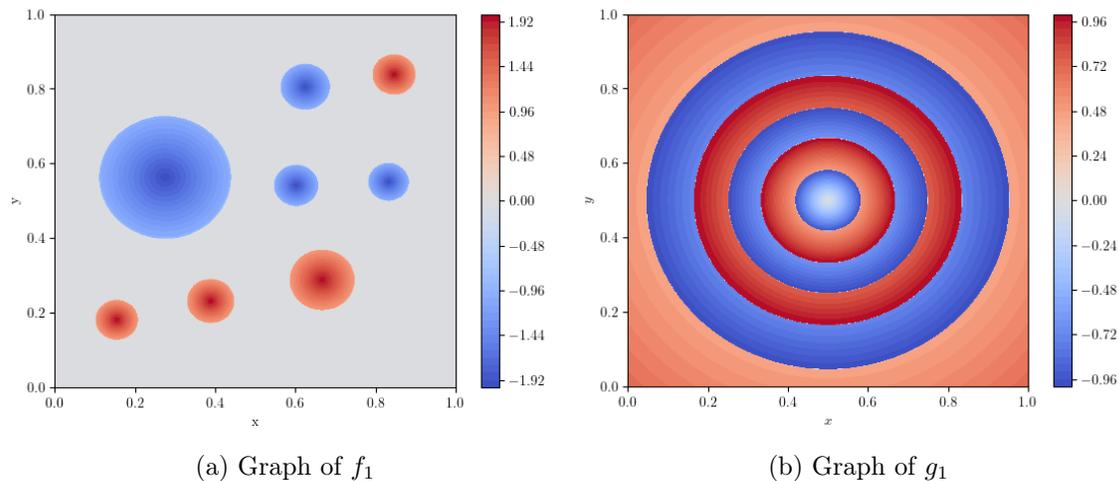

(a) Graph of f_1 (b) Graph of g_1

Figure 10: Graph of f_1 and g_1.

- First, we consider $k = 8$ non-intersecting discs $D_1, ..., D_k$, chosen randomly (random centers $(x_1, y_1), ..(x_k, y_k)$ and random radii $r_1, ..., r_k$) in $[0, 1]^2$. We also ensure that $D_1, ..., D_k$ do not intersect the boundary of $[0, 1]^2$. We then consider the family of signal $f_\alpha : [0, 1]^2 \to \mathbb{R}$, $\alpha \in]0, 1]$ defined by:

$$f_\alpha(x) = \begin{cases} (-1)^i \left(2 - \left(\frac{||x - x_i||_2}{r_i} \right)^\alpha \right) & \text{if } x \in D_i, 1 \leq i \leq k \\ 0 & \text{else} \end{cases}.$$

These are simply sums of bump functions with exponent α on the discs $D_1, ..., D_k$, shifted to create discontinuity at the boundaries of each $D_1, ..., D_k$. Note that f_α belongs to $S_2(M, L, R, \alpha)$, for, $M = 2$, $L = (1/\min_{1 \leq i \leq k} r_i)^\alpha$ and some $R > 0$ depending on $\min_{1 \leq i \leq k} r_i$ and the minimal distance of the discs $D_1, ..., D_k$ to the boundary of $[0, 1]^2$.

- Second, we choose $p = 5$ discs $\tilde{D}_1 \subset ... \subset \tilde{D}_p$ centered at $(0, 0)$ with raddii $1/2 > \tilde{r}_5 = 1/2.2 > \tilde{r}_4 = 1/3 > \tilde{r}_3 = 1/4 > \tilde{r}_2 = 1/6 > \tilde{r}_1 = 1/12$ and consider the family of signal $g_\alpha : [0, 1]^2 \to \mathbb{R}$, $\alpha \in]0, 1]$, defined by:

$$g_\alpha(x) = \begin{cases} -\left(\frac{||x - x_i||_2}{\tilde{r}_1} \right)^\alpha & \text{if } x \in \tilde{D}_1 \\ (-1)^i \left(\frac{||x - x_i||_2}{\tilde{r}_i} \right)^\alpha & \text{if } x \in \tilde{D}_i \setminus \tilde{D}_{i-1}, 2 \leq i \leq p \\ ||x - x_i||_2^\alpha & \text{else} \end{cases}.$$

28

In contrast to the previous example, where the objects in the image (represented by the disks $D_1, \ldots, D_k$) are non-overlapping, now, we consider k overlapping objects (represented by the disks $\tilde{D}_1, \ldots, \tilde{D}_p$) that are strictly contained within one another. This inclusion ensures that their boundaries do not intersect. As a result, it follows that g_α belongs to $S_2(M, L, R, \alpha)$, for $M = 1$, $L = (1/\min_{1 \leq i \leq k} \tilde{r}_i)^\alpha$, and some $R > 0$ depending on $\min(\tilde{r}_1, \tilde{r}_2 - \tilde{r}_1, \ldots, \tilde{r}_p - \tilde{r}_{p-1})$ and the distance of the disks $\tilde{D}_p$ to the boundary of $[0, 1]^2$.

For these two examples, we run simulations to illustrate that, although the estimation of the signals in the sup-norm is out of reach, the plug-in histogram estimators of their persistence diagrams are consistent. To achieve this, for varying resolutions of observations $\{N \times N, N \in [10 : 50 : 510]\}$ (where $[N_1 : q : N_2]$ denotes the set $\{N_1, N_1+q, N_1+2q, ..., N_2\}$), we generate noisy versions of the images associated with f_α and g_α by adding independent Gaussian noise to each pixel, with a standard deviation of $\sigma = 0.1$. We then estimate the signal via histograms. We choose the window size according to Theorem 1, taking $h = \frac{1}{10} \times (\ln(n)/n)^{1/(2\alpha+d)}$, and compute the diagrams associated to its sublevel sets using the Python package GUDHI (2025) via its function CUBICALCOMPLEX (Dlotko, 2025).

We repeat each simulation $r = 100$ times, from which we compute the average errors for both the bottleneck distance on the persistence diagrams and the sup-norm loss on the signals for each resolution. The true persistence diagrams are provided explicitly, whereas the sup-norm error is approximated by looking at the maximal errors on a grid with significantly higher resolution of 800×800. To examine the influence of regularity, we perform these simulations for several values of α: $\alpha = 1$, $\alpha = \frac{7}{8}$, $\alpha = \frac{2}{3}$, and $\alpha = \frac{1}{2}$.

The results are presented in Figure 11 for f_α and Figure 12 for g_α. They clearly show that the estimation of the signal is not consistent. This is intuitive because, at the pixels overlapping on the boundaries of the disks, consistent estimation is infeasible due to the discontinuity. However, we observe that the persistence diagrams are well-estimated, with errors in the bottleneck distance relatively rapidly converging to 0. This illustrates the inefficiency of the sup-norm stability theorems in these contexts, highlighting the relevance of the analysis we conducted.

Additionally, we compute the time required for each persistence diagram computation and calculate the average time for each resolution and each α. The results are shown in Table 1. The observed computation times appear reasonable, even for the highest resolutions. For these simulations, we consider relatively high regularity parameters α, but we still observe that computation times grow rapidly as the regularity decreases. In cases where regularity is low and resolution is high, using the theoretically optimal window h may become impractical, leading to a tradeoff between statistical performance and computational cost.

| | | **Resolution** | | | | | |
		10×10	110×110	210×210	310×310	410×410	510×510
α	1	$9,62 \times 10^{-4}$	$7,40 \times 10^{-2}$	$2,06 \times 10^{-1}$	$4,57 \times 10^{-1}$	$8,18 \times 10^{-1}$	$1,25$
	7/8	$1,06 \times 10^{-3}$	$7,11 \times 10^{-2}$	$2,69 \times 10^{-1}$	$4,46 \times 10^{-1}$	$9,88 \times 10^{-1}$	$1,16$
	2/3	$9,71 \times 10^{-4}$	$7,25 \times 10^{-2}$	$2,76 \times 10^{-1}$	$6,32 \times 10^{-1}$	$1,47$	$1,71$
	1/2	$1,24 \times 10^{-4}$	$1,90 \times 10^{-1}$	$2,90 \times 10^{-1}$	$6,51 \times 10^{-1}$	$1,49$	$2,44$

Table 1: Average computation time (in seconds) for computing the persistence diagram of f_α over $r = 100$ simulations, for varying resolutions and values of α.
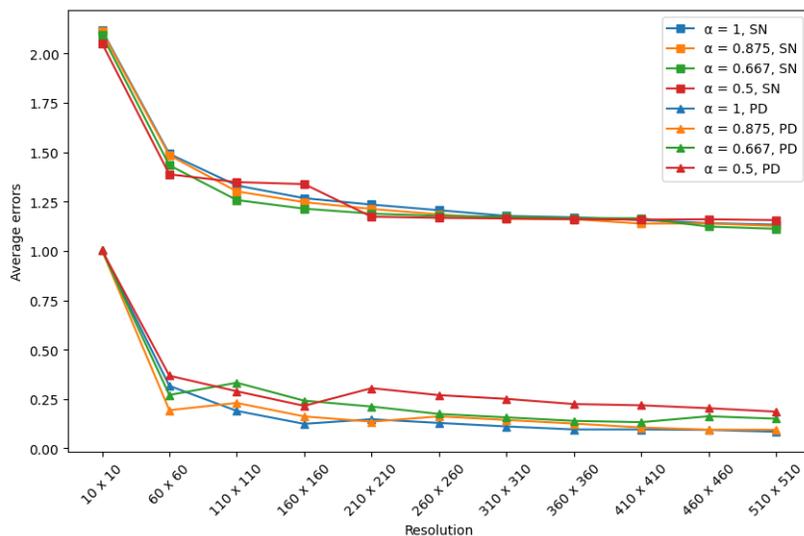
Figure 11: Simulation results for f_α. The average bottleneck distance errors for diagram estimation (PD, marked with triangles) and average sup norm errors for signal estimation (SN, marked with squares) are displayed as functions of the observation resolution. The red curves correspond to $\alpha = 0.5$, the green to $\alpha = 2/3$, the orange to $\alpha = 7/8$, and the blue to $\alpha = 1$
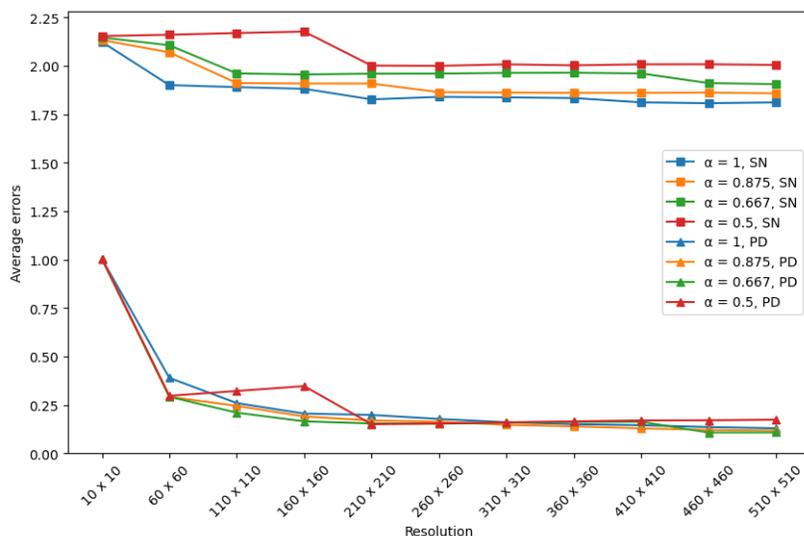

Figure 12: Simulation results for g_α. The average bottleneck distance errors for diagram estimation (PD, marked with triangles) and average sup norm errors for signal estimation (SN, marked with squares) are displayed as functions of the observation resolution for g_α. The red curves correspond to $\alpha = 0.5$, the green to $\alpha = 2/3$, the orange to $\alpha = 7/8$, and the blue to $\alpha = 1$.

30

6. Discussion

To date, the statistical analysis of persistence diagrams has largely depended on transferring established results from signal or density estimation, leveraging sup-norm stability. In contrast, the present work marks a departure from this paradigm. We introduce a finer statistical analysis of the plug-in histogram estimator, demonstrating that it achieves the minimax convergence rates over the classes $S_d(M, L, \alpha, R)$, matching the known rates for Hölder-continuous signals. These functional classes encompass irregular signals that typically pose significant challenges for classical nonparametric methods. It is also worth noting that the statistical arguments used in this work are limited to a simple concentration bound (Lemma 5), and can therefore be easily adapted to other standard models, such as the density estimation model or the Gaussian white noise model.

Beyond the theoretical results established in this work, our approach opens up a broader perspective on the inference of persistent homology. In particular, it reveals that the regularity assumptions traditionally imposed on the underlying signals can be meaningfully relaxed. This motivates further exploration of potential relaxations, especially of Assumption **A3**.

One promising direction involves controlling the μ-reach, as introduced in Chazal et al. (2006), of the discontinuity set. Such an extension would significantly broaden the applicability of our results, enabling the treatment of signals with more complex discontinuity structures, such as sets containing multiple points (e.g., self-intersections) or corners. In the context of image analysis, as discussed in Section 5, this would allow us to consider objects with intersecting boundaries, boundaries intersecting the image frame, and objects with non-smooth boundaries.

However, as illustrated in Figure 13, the plug-in histogram estimator becomes inadequate in these more complex settings. Histograms may fail to capture accurately the topology of sublevel sets or may create false topological features due to multiple points and intersections with the boundary of the cube. We believe this limitation is not unique to histograms but likely extends to other standard plug-in estimators. Addressing these challenges may require moving beyond the plug-in framework, calling for the development of new inference techniques.

Acknowledgements
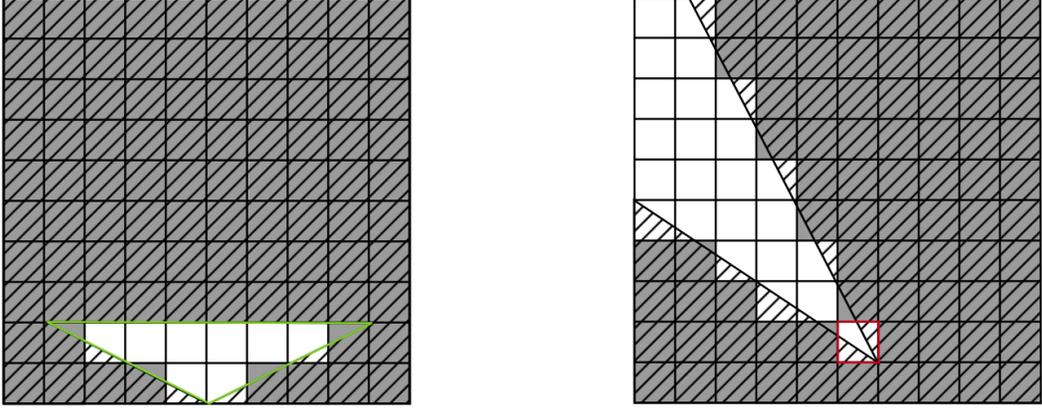
(a) A true cycle not captured by cubical approximation

(b) A false cycle created by cubical approximation

Figure 13: λ-sublevel cubical approximation for f, the function defined as 0 on the hatched area and K outside (for arbitrarily large K). (a) displays a case where the histogram approximation fails to capture the true cycle in green, for at least all $0 < \lambda < K/2$. (b) displays a case where the histogram approximation creates a cycle in red, not corresponding to any true cycle, with an arbitrarily long lifetime.

Appendix A. Proofs for $q-$tameness

This section is devoted to proving the claim that the persistence diagrams we considered in this work are well-defined. Following the construction of Chazal et al. (2016), it suffices to prove that the associated persistence modules are $q-$tame.

Definition 10 *A persistence module $\mathbb{V}$ is said to be q-tame if for all $\lambda < \lambda' \in \Lambda$, $\mathrm{rank}\left(v_\lambda^{\lambda'}\right)$ is finite.*

Lemma 6 *Let $f \in S_d(M, L, \alpha, R)$. For all $s \in \mathbb{N}$ and $h < \frac{R}{2}$, for all $\lambda \in \mathbb{R}$, there exists a morphism ϕ_λ such that*

$$
\begin{array}{ccc}
H_s\left(\mathcal{F}_\lambda\right) & \longrightarrow & H_s\left(\mathcal{F}_{\lambda+L(1+3^\alpha)h^\alpha}\right) \\
& \searrow & \nearrow \phi_\lambda \\
& H_s\left(\mathcal{F}_\lambda^h\right) &
\end{array}
\tag{16}
$$

is a commutative diagram (unspecified maps come from set inclusions).

Proof Let $\tilde{\phi}_\lambda : H_s\left(\mathcal{K}_{\lambda,h}\right) \to H_s\left(\mathcal{G}_{\lambda,h}\right)$ be the linear map induced by the deformation retraction from Lemma 2. We also denote $i_{1,\lambda} : H_s\left(\mathcal{F}_\lambda^h\right) \to H_s\left(\mathcal{K}_{\lambda,h}\right)$ the linear map induced by the inclusion $\mathcal{F}_\lambda^h \subset \mathcal{K}_{\lambda,h}$ and $i_{2,\lambda} : H_s\left(\mathcal{G}_{\lambda,h}\right) \to H_s\left(\mathcal{F}_{\lambda+L(1+3^\alpha)h^\alpha}\right)$ the linear map induced by the inclusion $\mathcal{G}_{\lambda,h} \subset \mathcal{F}_{\lambda+L(1+3^\alpha)h^\alpha}$, also provided by Lemma 2. We take

32

$\phi_\lambda = i_{2,\lambda} \circ \tilde{\phi}_\lambda \circ i_{1,\lambda}$. Diagram 16 then is (unspecified maps are induced by set inclusion),

$$
\begin{array}{ccc}
H_s\left(\mathcal{F}_\lambda\right) & \longrightarrow & H_s\left(\mathcal{F}_{\lambda+L(1+3^\alpha)h^\alpha}\right) \\[2ex]
\big\downarrow (F1) \qquad (F2) \qquad (F3) & & \big\uparrow i_{2,\lambda} \\[2ex]
H_s\left(\mathcal{F}_\lambda^h\right) \xrightarrow{\ i_{1,\lambda}\ } H_s\left(\mathcal{K}_{\lambda,h}\right) \xleftarrow{\ \tilde{\phi}_\lambda\ } & & H_s\left(\mathcal{G}_{\lambda,h}\right)
\end{array}
\tag{17}
$$

Faces $(F1)$ and $(F3)$ simply commutes by inclusion. Face $(F2)$ commutes as $\tilde{\phi}_\lambda$ is induced by a deformation retraction. All faces of Diagram 17 commute, hence Diagram 17 (and equivalently Diagram 16) is commutative. ∎

Proposition 1 *Let $f \in S_d(M, L, \alpha, R)$ then f is q-tame.*

Proof Let $s \in \mathbb{N}$ and $\mathbb{V}_{s,f}$ be the persistence module (for the $s-$th homology) associated to the sublevel sets filtration $\mathcal{F}$. For fixed levels $\lambda < \lambda'$ denote $v_\lambda^{\lambda'}$ the associated map. Let $\lambda \in \mathbb{R}$ and $h < \frac{R}{2}$. By Lemma 6, $v_\lambda^{\lambda+L(1+3^\alpha)h^\alpha} = \phi_\lambda \circ \tilde{i}_\lambda$, with $\tilde{i}_\lambda : H_s\left(\mathcal{F}_\lambda\right) \to H_s\left(\mathcal{F}_\lambda^h\right)$. By Assumptions **A1** and **A2**, $\mathcal{F}_\lambda$ is compact. As $[0,1]^d$ is triangulable, $\mathcal{F}_\lambda$ is covered by finitely many cells of the triangulation, there is a finite simplicial complex K such that $\overline{\mathcal{F}_\lambda} \subset K \subset \mathcal{F}_\lambda^h$. Consequently, $\tilde{i}_\lambda$ factors through the finite-dimensional space $H_s(K)$ and is then of finite rank. Thus, $v_\lambda^{\lambda+L(1+3^\alpha)^\alpha h^\alpha}$ is of finite rank for all $0 < h < \frac{R}{2}$. As for any $\lambda < \lambda' < \lambda''$, $v_\lambda^{\lambda''} = v_{\lambda'}^{\lambda''} \circ v_\lambda^{\lambda'}$, we have that $v_\lambda^{\lambda'}$ is of finite rank for all $\lambda < \lambda'$. Hence, f is q-tame. ∎

Proposition 2 *Let $f \in S_d(M, L, \alpha, R)$ then, for all $s \in \mathbb{N}$, $\widehat{\mathbb{V}}_{s,f}^h$ is q-tame.*

Proof Let $h > 0$ and $\lambda \in \mathbb{R}$. $\widehat{\mathcal{F}}_\lambda$ is a union of hypercubes of the regular grid G_h, thus, $H_s\left(\widehat{\mathcal{F}}_\lambda\right)$ is finite dimensional. Thus, $\widehat{\mathbb{V}}_{s,f}$ is q-tame by Theorem 1.1 of Crawley-Boevey (2012). ∎

Appendix B. Proofs of Technical Lemmas

B.1 Proof of Lemma 1

This section is dedicated to the proof of Lemma 1, from Section 3, which relies on the following lemma.

Lemma 7 *Let $f : [0,1]^d \to \mathbb{R}$ and h satisfying (1). Let $H \subset \mathcal{F}_{\lambda+\sqrt{2}\sigma N_h h^\alpha}^c \cap C_h$ and $H' \subset \mathcal{F}_{\lambda-\sqrt{2}\sigma N_h h^\alpha} \cap C_h$. We have that:*

$$
\frac{1}{nh^d} \sum_{x_i \in H} X_i > \lambda \ \text{ and } \ \frac{1}{nh^d} \sum_{x_i \in H'} X_i < \lambda.
$$

Proof Let us consider here the case where in $H' \subset \mathcal{F}_{\lambda - \sqrt{2}\sigma N_h h^\alpha}$ (the proof being the same in both cases). We have:

$$\frac{1}{nh^d} \sum_{x_i \in H'} X_i$$

$$= \frac{1}{nh^d} \sum_{x_i \in H'} f(x_i) + \sigma\varepsilon_i$$

$$\leq \lambda - \sqrt{2}\sigma N_h h^\alpha + N_h\sqrt{2}\sigma\sqrt{\frac{\log(1/h^d)}{nh^d}}$$

$$< \lambda$$

By the choice made for h. ∎

Proof [Proof of Lemma 1] Let $x \in \mathcal{F}_{\lambda - \sqrt{2}\sigma N_h h^\alpha}^{-\sqrt{d}h}$ and H be the hypercube of C_h containing x. We then have:

$$H \subset \mathcal{F}_{\lambda - \sqrt{2}\sigma N_h h^\alpha}.$$

Hence, by Lemma 7, $\sum_{x_i \in H} X_i - nh^d\lambda < 0$, thus,

$$H \subset \widehat{\mathcal{F}}_\lambda.$$

Now, let $x \in \left(\mathcal{F}_{\lambda + \sqrt{2}\sigma N_h h^\alpha}^{\sqrt{d}h}\right)^c$, and H be the hypercube of C_h containing x. We then have:

$$H \subset \mathcal{F}_{\lambda + \sqrt{2}\sigma N_h h^\alpha}^c.$$

Hence, by Lemma 7, $\sum_{x_i \in H} X_i - nh^d\lambda > 0$, thus,

$$H \subset \widehat{\mathcal{F}}_\lambda^c$$

and Lemma 1 is proved. ∎

B.2 Proof of Lemma 2

This section is devoted to the proof of Lemma 2 from Section 3.

Proof First, note that if x belongs to $\bigcup_{x \in S_{\lambda,h}} [x, \xi(x)]$ then x is at distance at most h from the union of $(\partial M_i)_{i=1,\ldots,l}$, and thus $||x - \xi(x)||_2 \leq h$ which proves that $\mathcal{K}_{\lambda,h} \subset \mathcal{F}_\lambda^{2h}$. As $\mathcal{F}_\lambda \subset \left(\bigcup_{x \in S_{\lambda,h}} [x, \xi(x)]\right)^c \cap \mathcal{F}_\lambda^h$, $\mathcal{F}_\lambda \subset \mathcal{G}_{\lambda,h}$.

Now, we prove that $F_{\lambda,h}$ is a deformation retraction. By definition of $\mathcal{G}_{\lambda,h}$:

$$F_{\lambda,h}(x,1) \in \mathcal{G}_{\lambda,h}, \quad \forall x \in \mathcal{K}_{\lambda,h}$$

and by definition of $F_{\lambda,h}$:

$$F_{\lambda,h}(x,0) = x, \quad \forall x \in \mathcal{K}_{\lambda,h}$$

Let $x \in \mathcal{K}_{\lambda,h}$ satisfying (2) and (3), we have $F_{\lambda,h}(x,t) \in [x, \xi(x)]$ for all $t \in [0,1]$. In particular, this implies that $\xi(F_{\lambda,h}(x,1)) = \xi(x)$ thus, by definition of $F_{\lambda,h}$, $F_{\lambda,h}(F_{\lambda,h}(x,1),1) = F_{\lambda,h}(x,1)$. Otherwise, $F_{\lambda,h}(x,1) = x$. Hence,

$$F_{\lambda,h}(x,1) = x, \quad \forall x \in \mathcal{G}_{\lambda,h}.$$

The proof for the continuity of $F_{\lambda,h}$ is provided separately in Appendix B.3. Then $F_{\lambda,h}$ is a deformation retraction of $\mathcal{K}_{\lambda,h}$ onto $\mathcal{G}_{\lambda,h}$.

Now, we prove that $\mathcal{G}_{\lambda,h} \subset \mathcal{F}_{\lambda+(1+3^\alpha)Lh^\alpha}$. Let $x \in \mathcal{K}_{\lambda,h}$, and suppose that $x \in \overline{M}_i \cap [0,1]^d$:

- If x does not satisfy (2), $F_{\lambda,h}(x,1) = x$, then, directly, by definition of $S_{\lambda,h}$, x belongs $\mathcal{F}_{\lambda+Lh^\alpha}$.

- If x satisfies (2) and $2h - d_2\left(\xi(x), M_i \cap \mathcal{F}_{\lambda+Lh^\alpha}\right) \geq 0$, as $F_{\lambda,h}(x,1) \in [x, \xi(x)] \subset \overline{M}_i$, we have

$$d_2\left(F_{\lambda,h}(x,1), M_i \cap \mathcal{F}_{\lambda+Lh^\alpha}\right) \leq 3h.$$

Thus, Assumptions **A1** and **A2** then ensure that (details concerning this claim are provided in Lemma 12, Appendix C.2),

$$F_{\lambda,h}(x,1) \in \mathcal{F}_{\lambda+L(1+3^\alpha)h^\alpha}.$$

- If x satisfies (2) and $2h - d_2\left(\xi(x), M_i \cap \mathcal{F}_{\lambda+Lh^\alpha}\right) < 0$, then, $F_{\lambda,h}(x,1) = \xi(x)$. Let $\varepsilon > 0$, there exist $j \in \{1, ..., l\}$, $i \neq j$ and $y \in \mathcal{F}_\lambda \cap M_j$, such that $\|x - y\|_2 \leq h + \varepsilon$. Hence, $\xi(x) \in \partial M_j \cap]0,1[^d$ and $\|\xi(x) - y\|_2 \leq 2h + \varepsilon$. Assumptions **A1** and **A2** then ensure that (see again Lemma 12 in Appendix C.2),

$$\xi(x) \in \mathcal{F}_{\lambda+L(1+(2+\varepsilon)^\alpha)h^\alpha}$$

as it holds for all $\varepsilon > 0$,

$$F_{\lambda,h}(x,1) = \xi(x) \in \mathcal{F}_{\lambda+L(1+2^\alpha)h^\alpha}.$$

Finally, combining cases, $\mathcal{G}_{\lambda,h} \subset \mathcal{F}_{\lambda+L(1+3^\alpha)h^\alpha}$. ∎

B.3 Proof of the Continuity of $F_{\lambda,h}$

This section is devoted to the proof of $F_{\lambda,h}$, claimed in the proof of Lemma 2.

Lemma 8 *Let $R/2 > h > 0$ and $\lambda \in \mathbb{R}$, $F_{\lambda,h}$ is continuous.*

Proof Let $\delta, \delta' > 0$, $x, y \in \mathcal{K}_{\lambda,h}$ such that $\|x - y\|_2 \leq \delta$ and $t, s \in [0,1]$ such that $|t - s| \leq \delta'$. Let's check the different cases.

We begin with the cases where $x \in \overline{M}_i$ and $y \in \overline{M}_j$, $i \neq j$. Let $\delta < h$, then $\|x - \xi(x)\|_2 \leq \delta$, $\|y - \xi(y)\|_2 \leq \delta$, and thus $F_{\lambda,h}(x,t), F_{\lambda,h}(y,s) \in [x, \xi(x)] \cup [y, \xi(y)] \subset B_2(x, 2\delta)$. Then,

$$\|F_{\lambda,h}(x,t) - F_{\lambda,h}(y,s)\|_2 \leq 4\delta$$

And the conclusion follows in this case. From now on, we suppose that $x, y \in M_i$.

- If x does not satisfy (2) or (3) and y does not satisfy (2) or (3), then, directly,

$$||F_{\lambda,h}(x,t) - F_{\lambda,h}(y,s)||_2 = ||x - y||_2 \leq \delta.$$

- If x satisfies (2) and (3), and y does not satisfy (2), then, $y \in \mathcal{F}_{\lambda+Lh^\alpha}$. Thus,

$$d_2\left(\xi(x), M_i \cap \mathcal{F}_{\lambda+Lh^\alpha}\right) \leq ||x - \xi(x)|| + ||x - y||_2$$

and thus, by (3),

$$||x - \xi(x)|| \geq 2h - d_2\left(\xi(x), M_i \cap \mathcal{F}_{\lambda+Lh^\alpha}\right) \geq ||x - \xi(x)|| - \delta.$$

Consequently,

$$\left\|\xi(x) + (2h - d_2\left(\xi(x), M_i \cap \mathcal{F}_{\lambda+Lh^\alpha}\right))_+ \frac{x - \xi(x)}{||x - \xi(x)||_2} - x\right\|_2 \leq \delta$$

Then,

$$||F_{\lambda,h}(x,t) - F_{\lambda,h}(y,s)||_2$$
$$= \left\|(1-t)x + t\left(\xi(x) + (2h - d_2\left(\xi(x), M_i \cap \mathcal{F}_{\lambda+Lh^\alpha}\right))_+ \frac{x - \xi(x)}{||x - \xi(x)||_2}\right) - y\right\|_2$$
$$\leq ||x - y||_2 \quad + \left\|\xi(x) + (2h - d_2\left(\xi(x), M_i \cap \mathcal{F}_{\lambda+Lh^\alpha}\right))_+ \frac{x - \xi(x)}{||x - \xi(x)||_2} - x\right\|_2$$
$$\leq 2\delta.$$

- If x satisfies (2) and (3), and y satisfies (2) but not (3). Then,

$$||x - \xi(x)||_2 \geq 2h - d_2\left(\xi(x), M_i \cap \mathcal{F}_{\lambda+Lh^\alpha}\right)$$
$$= 2h - d_2\left(\xi(y), M_i \cap \mathcal{F}_{\lambda+Lh^\alpha}\right)$$
$$\quad + d_2\left(\xi(y), M_i \cap \mathcal{F}_{\lambda+Lh^\alpha}\right) - d_2\left(\xi(x), M_i \cap \mathcal{F}_{\lambda+Lh^\alpha}\right)$$
$$\geq 2h - d_2\left(\xi(y), M_i \cap \mathcal{F}_{\lambda+Lh^\alpha}\right) - ||\xi(x) - \xi(y)||_2$$
$$\geq ||y - \xi(y)||_2 - ||\xi(x) - \xi(y)||_2$$
$$\geq ||x - \xi(x)||_2 - 2||\xi(x) - \xi(y)||_2 - ||x - y||_2.$$

Hence,

$$\left\|\xi(x) + (2h - d_2\left(\xi(x), M_i \cap \mathcal{F}_{\lambda+Lh^\alpha}\right))_+ \frac{x - \xi(x)}{||x - \xi(x)||_2} - x\right\|_2$$
$$\leq ||x - y||_2 + 2||\xi(x) - \xi(y)||_2.$$

And thus, we have:

$$||F_{\lambda,h}(x,t) - F_{\lambda,h}(y,s)||_2$$
$$= \left\|(1-t)x + t\left(\xi(x) + (2h - d_2\left(\xi(x), M_i \cap \mathcal{F}_{\lambda+Lh^\alpha}\right))_+ \frac{x - \xi(x)}{||x - \xi(x)||_2}\right) - y\right\|_2$$

$$\leq ||x - y||_2 \quad + \left\| \xi(x) + (2h - d_2\left(\xi(x), M_i \cap \mathcal{F}_{\lambda + Lh^\alpha}\right))_+ \frac{x - \xi(x)}{||x - \xi(x)||_2} - x \right\|_2$$

$$\leq 2||x - y||_2 + 2||\xi(x) - \xi(y)||_2$$

$$\leq 2\delta + 2||\xi(x) - \xi(y)||_2$$

and we conclude by continuity of ξ.

- Finally, if x and y both satisfy (2) and (3), then,

$$||F_{\lambda,h}(x,t) - F_{\lambda,h}(y,s)||_2$$

$$= \left\| (1-t)x + t\left(\xi(x) + (2h - d_2\left(\xi(x), M_i \cap \mathcal{F}_{\lambda+Lh^\alpha}\right))_+ \frac{x - \xi(x)}{||x - \xi(x)||_2} \right) \right.$$

$$\left. - (1-s)y - s\left(\xi(y) + (2h - d_2\left(\xi(y), M_i \cap \mathcal{F}_{\lambda+Lh^\alpha}\right))_+ \frac{y - \xi(y)}{||y - \xi(y)||_2} \right) \right\|_2$$

and the conclusion follows again, in this case by continuity of ξ.

All possible cases have been checked, the proof is complete. ∎

B.4 Proof of Lemma 3

This section is dedicated to proof of Lemma 3 from Section 3.

Proof [Proof of Lemma 3] First, we check that γ_h extends continuously to $P_{\lambda,h}$. Let $x \in P_{\lambda,h} \cap \bigcup_{i=1}^l \partial M_i \cap]0,1[^d$. Assumption **A3** ensures that $P_{\lambda,h} \subset]0,1[^d$, and that there exist $i,j \in \{1,\ldots,l\}$ such that $B_2(x,h) \subset M_i \cup M_j \cup (\partial M_i \cap \partial M_j)$ (details concerning this claim are provided in Appendix C.1). Now, if

$$B_2(x,h) \cap \mathcal{F}_\lambda \cap M_i \neq \emptyset \text{ and } B_2(x,h) \cap \mathcal{F}_\lambda \cap M_j \neq \emptyset$$

then by Assumptions **A2** and **A1**, $B_2(x,h) \subset \mathcal{F}_{\lambda+L2h^\alpha}$ (see Lemma 12 in Appendix C.2) and thus $x \in \mathcal{F}_{\lambda+L2h^\alpha}^{-h}$. Hence, $B_2(x,h) \cap P_{\lambda,h} \cap M_j = \emptyset$ or $B_2(x,h) \cap P_{\lambda,h} \cap M_i = \emptyset$. Without loss of generality, suppose that $B_2(x,h) \cap P_{\lambda,h} \cap M_j = \emptyset$. Assumption **A3** imposes that $\bigcup_{i=1}^l \partial M_i \cap]0,1[^d$ is a $C^{1,1}$ hypersurface and thus ensures that, for all $x \in P_{\lambda,h} \cap \overline{M}_i \cap]0,1[^d$, $\lim_{y \in M_i \cap P_{\lambda,h} \to x} \gamma_h(y)$ exists. We can then define:

$$\gamma_{h,\lambda}(x) = \lim_{y \in M_i \cap P_{\lambda,h} \to x} \gamma_h(y).$$

Note that this intuitively follows from the fact that the $C^{1,1}$ assumption ensures that the normal cone of $\bigcup_{i=1}^l \partial M_i \cap]0,1[^d$ at $\xi(x)$, which contains the set of points $\{y \in P_{\lambda,h}, \xi(y) = \xi(x)\}$ by Theorem 4.8 of Federer (1959), is simply a line. Thus, there is only one point at distance h from $\xi(x)$ in $\{y \in \overline{M}_i \cap P_{\lambda,h}, \xi(y) = \xi(x)\}$, namely $\gamma_{h,\lambda}(x)$. Doing so for all $x \in P_{\lambda,h} \cap \bigcup_{i=1}^l \partial M_i \cap]0,1[^d$ extends continuously $\gamma_h(x)$ to $P_{\lambda,h}$.

Now, we prove that $H_{\lambda,h}$ is a deformation retraction. As $\mathcal{F}_\lambda^{-h} \subset \left(\bigcup_{x \in P_{\lambda,h}} [x, \gamma_{h,\lambda}(x)] \right)^c \cap \mathcal{F}_\lambda$, $\mathcal{F}_\lambda^{-h} \subset \mathcal{M}_{\lambda,h}$. Note that, by definition of $\mathcal{M}_{\lambda,h}$,

$$H_{\lambda,h}(x,1) \in \mathcal{M}_{\lambda,h}, \quad \forall x \in \mathcal{N}_{\lambda,h}$$

and by definition of $H_{\lambda,h}$

$$H_{\lambda,h}(x,0) = x, \quad \forall x \in \mathcal{N}_{\lambda,h}$$

Let $x \in \mathcal{N}_{\lambda,h}$ satisfying (4) and (5). By construction $H_{\lambda,h}(x,t) \in [x, \gamma_{h,\lambda}(x)]$ for all $t \in [0,1]$. In particular, this implies that $\gamma_{\lambda,x}(H_{\lambda,h}(x,1)) = \gamma_{h,\lambda}(x)$. Thus, $H_{\lambda,h}(H_{\lambda,h}(x,1),1) = H_{\lambda,h}(x,1)$. In other cases $H_{\lambda,h}(x,1) = x$. Hence,

$$H_{\lambda,h}(x,1) = x, \quad \forall x \in \mathcal{M}_{\lambda,h}.$$

The proof of the continuity of $H_{\lambda,h}$ is provided separately in Appendix B.5. Then $H_{\lambda,h}$ is a deformation retraction of $\mathcal{N}_{\lambda,h}$ onto $\mathcal{M}_{\lambda,h}$.

Now, we prove that $\mathcal{M}_{\lambda,h} \subset \mathcal{F}_{\lambda+L(2+5\alpha)h^\alpha}^{-h}$. Let $x \in \mathcal{N}_{\lambda,h}$, and suppose that $x \in \overline{M}_i \cap [0,1]^d$:

- If x does not satisfy (4), directly, $F(1,x) = x \in \mathcal{F}_{\lambda+2Lh^\alpha}^{-h}$.

- If x satisfies (4) and $3h - d_2\left(\gamma_{h,\lambda}(x), (\overline{M}_i)^c \cap \mathcal{F}_{\lambda+2Lh^\alpha}\right) \geq 0$, then there exists $z \in M_j \cap \mathcal{F}_{\lambda+2Lh^\alpha}$ with $j \neq i$ such that $||x - z||_2 \leq 3h$ thus $||H_{\lambda,h}(x,1) - z||_2 \leq 4h$. By Assumption **A3**, $B_2(H_{\lambda,h}(x,1),h) \subset \overline{M}_i \cup \overline{M}_j$ (see Lemma 11 in Appendix C.1) and by Assumptions **A1** and **A2** (see Lemma 12 in Appendix C.2):

$$B_2(H_{\lambda,h}(x,1),h) \cap \overline{M}_j \subset B_2(z,5h) \cap \overline{M}_j \subset \mathcal{F}_{\lambda+L(2+5\alpha)h^\alpha}$$

and

$$B_2(H_{\lambda,h}(x,1),h) \cap \overline{M}_i \subset B_2(x,2h) \subset \mathcal{F}_{\lambda+L3^\alpha h^\alpha}.$$

Thus, it follows that:

$$H_{\lambda,h}(x,1) \in \mathcal{F}_{\lambda+L(2+5\alpha)h^\alpha}^{-h}.$$

- If x satisfies (4) and $3h - d_2\left(\gamma_{h,\lambda}(x), (\overline{M}_i)^c \cap \mathcal{F}_{\lambda+2Lh^\alpha}\right) < 0$, then $H_{\lambda,h}(x,1) = \gamma_{h,\lambda}(x)$ and thus $B_2(H_{\lambda,h}(x,1),h) \subset \overline{M}_i$. As $||x - \gamma_{h,\lambda}(x)||_2 \leq h$, it follows, by Assumptions **A1** and **A2** (see again Lemma 12 in Appendix C.2), that

$$H_{\lambda,h}(x,1) \in \mathcal{F}_{\lambda+L3^\alpha h^\alpha}^{-h}.$$

From the same reasoning, it also follows that $[x, \gamma_{h,\lambda}(x)] \subset \mathcal{F}_{\lambda+Lh^\alpha}$ and hence $\mathcal{N}_{\lambda,h} \subset \mathcal{F}_{\lambda+Lh^\alpha}$.

Combining the different cases, it follows that $\mathcal{M}_{\lambda,h} \subset \mathcal{F}_{\lambda+L(2+5\alpha)h^\alpha}^{-h}$. ∎

B.5 Proof of the Continuity of $H_{\lambda,h}$

This section is devoted to the proof of the continuity of $H_{\lambda,h}$, claimed in the proof of Lemma 3.

Lemma 9 *Let $R/2 > h > 0$ and $\lambda \in \mathbb{R}$, $H_{\lambda,h}$ is continuous.*

Proof Let $\delta, \delta' > 0$, $x, y \in \mathcal{N}_{\lambda,h}$ such that $||x - y||_2 \leq \delta$ and $t, s \in [0,1]$ such that $|t - s| \leq \delta'$. Let's check the different cases.

- If $x \in \overline{M}_i$, $\gamma_{\lambda,h}(x) \in M_i$ and $\gamma_{\lambda,h}(y) \in \overline{M}_i^c$, then:

$$d_2\left(\gamma_{h,\lambda}(x), (\overline{M}_i)^c \cap \mathcal{F}_{\lambda+2Lh^\alpha}\right) \leq 2h + \delta.$$

Thus, either x satistifies (4) and (5) and we have :

$$||\gamma_{h,\lambda}(x) - x||_2 \geq 3h - d_2\left(\gamma_{h,\lambda}(x), (\overline{M}_i)^c \cap \mathcal{F}_{\lambda+2Lh^\alpha}\right) \geq ||\gamma_{h,\lambda}(x) - x||_2 - \delta$$

and consequently

$$\left\|\gamma_{h,\lambda}(x) + \left(3h - d_2\left(\gamma_{h,\lambda}(x), (\overline{M}_i)^c \cap \mathcal{F}_{\lambda+2Lh^\alpha}\right)\right)_+ \frac{x - \gamma_{h,\lambda}(x)}{||x - \gamma_{h,\lambda}(x)||_2} - x\right\|_2 \leq \delta.$$

which gives $||H_{\lambda,h}(x,t) - x||_2 \leq \delta$. Or, x does not satistify (4) or (5) and $H_{\lambda,h}(x,t) = x$. In both cases $||H_{\lambda,h}(x,t) - x||_2 \leq \delta$. Similarly we can show that $||H_{\lambda,h}(y,s) - y||_2 \leq \delta$. Hence,

$$||H_{\lambda,h}(x,t) - H_{\lambda,h}(y,s)||_2 \leq ||H_{\lambda,h}(x,t) - x||_2 + ||x - y||_2 + ||H_{\lambda,h}(y,s) - y||_2 \leq 3\delta.$$

From now on, we can suppose that $x, y \in \overline{M}_i$ and $\gamma_{\lambda,h}(x), \gamma_{\lambda,h}(y) \in M_i$.

- If x does not satisfy (4) or (5), and y does not satisfy (4) or (5), then directly,

$$||H_{\lambda,h}(x,t) - H_{\lambda,h}(y,s)||_2 = ||x - y||_2 \leq \delta.$$

- If x satisfies (4) and (5) and $y \notin ((\partial M_i \cap]0,1[^d)^h)^\circ$, then, $d_2\left(x, \partial M_i \cap]0,1[^d\right) \geq h - \delta$ and thus $||x - \gamma_{h,\lambda}(x)||_2 \leq \delta$. As $H_{\lambda,h}(x,t) \in [x, \gamma_{h,\lambda}(x)]$, we have:

$$||H_{\lambda,h}(x,t) - H_{\lambda,h}(y,s)||_2 = ||H_{\lambda,h}(x,t) - y||_2 \leq ||x - y||_2 + ||x - H_{\lambda,h}(x,t)||_2 \leq 2\delta.$$

- If x satisfies (4) and (5) and $y \in \left(\bigcup_{x \in P_{\lambda,h}} [x, \gamma_{h,\lambda}(x)]\right)^c \cap \left(\left(\partial M_i \cap]0,1[^d\right)^h\right)^\circ$. Then, $y \in \mathcal{F}_{\lambda+2Lh^\alpha}^{-h}$. Thus, for sufficiently small δ there exists $z \in (\overline{M}_i)^c \cap B_2(y,h)$ and,

$$d_2\left(\gamma_{h,\lambda}(x), (\overline{M}_i)^c \cap \mathcal{F}_{\lambda+2Lh^\alpha}\right) - 2h \leq ||\gamma_{h,\lambda}(x) - z||_2 - 2h \leq ||x - y||_2 \leq \delta.$$

Hence, by (5),

$$||\gamma_{h,\lambda}(x) - x||_2 \geq 3h - d_2\left(\gamma_{h,\lambda}(x), (\overline{M}_i)^c \cap \mathcal{F}_{\lambda+2Lh^\alpha}\right) \geq ||\gamma_{h,\lambda}(x) - x||_2 - \delta$$

and consequently,

$$\left\|\gamma_{h,\lambda}(x) + \left(3h - d_2\left(\gamma_{h,\lambda}(x), (\overline{M}_i)^c \cap \mathcal{F}_{\lambda+2Lh^\alpha}\right)\right)_+ \frac{x - \gamma_{h,\lambda}(x)}{||x - \gamma_{h,\lambda}(x)||_2} - x\right\|_2 \leq \delta.$$

We then have:

$$||H_{\lambda,h}(x,t) - H_{\lambda,h}(y,s)||_2$$
$$= ||(1-t)x + t\left(\gamma_{h,\lambda}(x)\right.$$

39

$$+ \left(3h - d_2\left(\gamma_{h,\lambda}(x), (\overline{M}_i)^c \cap \mathcal{F}_{\lambda+2Lh^\alpha}\right)\right)_+ \frac{x - \gamma_{h,\lambda}(x)}{||x - \gamma_{h,\lambda}(x)||_2}\right) - y\bigg\|_2$$

$$\leq \left\|\gamma_{h,\lambda}(x) + \left(3h - d_2\left(\gamma_{h,\lambda}(x), (\overline{M}_i)^c \cap \mathcal{F}_{\lambda+2Lh^\alpha}\right)\right)_+ \frac{x - \gamma_{h,\lambda}(x)}{||x - \gamma_{h,\lambda}(x)||_2} - x\right\|_2$$

$$+ ||x - y||_2$$

$$\leq 2\delta$$

- If x satisfies (4) and (5) and y satisfies (4) but not (5), then,

$$||\gamma_{h,\lambda}(x) - x||_2 \geq 3h - d_2\left(\gamma_{h,\lambda}(x), (\overline{M}_i)^c \cap \mathcal{F}_{\lambda+2Lh^\alpha}\right)$$
$$\geq ||y - \gamma_{h,\lambda}(y)||_2 - ||\gamma_{h,\lambda}(x) - \gamma_{h,\lambda}(y)||_2$$
$$\geq ||x - \gamma_{h,\lambda}(x)||_2 - 2||\gamma_{h,\lambda}(x) - \gamma_{h,\lambda}(y)||_2 - ||x - y||_2.$$

Thus,

$$||H_{\lambda,h}(x,t) - H_{\lambda,h}(y,s)||_2$$
$$= \|(1-t)x + t\left(\gamma_{h,\lambda}(x)\right.$$

$$\left. + \left(3h - d_2\left(\gamma_{h,\lambda}(x), (\overline{M}_i)^c \cap \mathcal{F}_{\lambda+2Lh^\alpha}\right)\right)_+ \frac{x - \gamma_{h,\lambda}(x)}{||x - \gamma_{h,\lambda}(x)||_2}\right) - y\bigg\|_2$$

$$\leq \left\|\gamma_{h,\lambda}(x) + \left(3h - d_2\left(\gamma_{h,\lambda}(x), (\overline{M}_i)^c \cap \mathcal{F}_{\lambda+2Lh^\alpha}\right)\right)_+ \frac{x - \gamma_{h,\lambda}(x)}{||x - \gamma_{h,\lambda}(x)||_2} - x\right\|_2$$

$$+ ||x - y||_2$$

$$\leq 2||\gamma_{h,\lambda}(x) - \gamma_{h,\lambda}(y)||_2 + 2||x - y||_2$$

$$\leq 2\delta + 2||\gamma_{h,\lambda}(x) - \gamma_{h,\lambda}(y)||_2$$

and we conclude, in this case, by continuity of $\gamma_{h,\lambda}$.

- Finally, if x satisfies (4) and (5) and y satisfies (4) and (5), then,

$$||H_{\lambda,h}(x,t) - H_{\lambda,h}(y,s)||_2$$
$$= \|(1-t)x - (1-s)y$$

$$+t\left(\gamma_{h,\lambda}(x) + \left(3h - d_2\left(\gamma_{h,\lambda}(x), (\overline{M}_i)^c \cap \mathcal{F}_{\lambda+2Lh^\alpha}\right)\right)_+ \frac{x - \gamma_{h,\lambda}(x)}{||x - \gamma_{h,\lambda}(x)||_2}\right)$$

$$-s\left(\gamma_{h,\lambda}(y) + \left(3h - d_2\left(\gamma_{h,\lambda}(y), (\overline{M}_i)^c \cap \mathcal{F}^{-h}_{\lambda+Lh^\alpha}\right)\right)_+ \frac{y - \gamma_{h,\lambda}(y)}{||y - \gamma_{h,\lambda}(y)||_2}\right)\bigg\|_2$$

and again the conclusion, follows in this case, by continuity of $\gamma_{h,\lambda}$.

All possible cases have been checked, the proof is complete. ∎

B.6 Proof of Lemma 4

This section is devoted to the proof of Lemma 4 from Section 3. The arguments for Assertions (6) and (7) rely on the same underlying ideas:

- First, due to Assumption **A3** (see details in Appendix C.1), in a sufficiently small neighborhood V of any point x close to the boundary of the pieces of f, the boundary locally corresponds to the frontier between two pieces M_i and M_j.

- Secondly, by Assumption **A3** again, this frontier can be well approximated (up to a quadratic error) by a hyperplane (see Figure 14).

We formalize this intuition in Lemma 10.

Lemma 10 *Let $0 < K$ and $0 < h < 1$ such that $Kh < R/2$. There exists a constant C_2 (depending only on K, d and R) such that for all $i, j \in \{1, ..., l\}$ and*

$$x \in B_2\left(\left(\partial M_i \cap]0, 1[^d\right), Kh\right) \cap \overline{M}_i$$

such that $\xi(x) \in \partial M_j$, we have:

$$d_2\left(B_2\left(\xi(x), Kh\right) \cap M_j, B_2\left(\xi(x), Kh\right) \cap \underline{P}(x)\right) \leq C_2 h^2 \tag{18}$$

with

$$\underline{P}(x) = \left\{z \in [0, 1]^d \text{ s.t. } \left\langle z, \frac{x - \xi(x)}{\|x - \xi(x)\|_2}\right\rangle \leq \left\langle \xi(x), \frac{x - \xi(x)}{\|x - \xi(x)\|_2}\right\rangle\right\}$$

and

$$d_2\left(B_2\left(\xi(x), Kh\right) \cap M_i, B_2\left(\xi(x), Kh\right) \cap \overline{P}(x)\right) \leq C_2 h^2 \tag{19}$$

with

$$\overline{P}(x) = \left\{z \in [0, 1]^d \text{ s.t. } \left\langle z, \frac{x - \xi(x)}{\|x - \xi(x)\|_2}\right\rangle \geq \left\langle \xi(x), \frac{x - \xi(x)}{\|x - \xi(x)\|_2}\right\rangle\right\}.$$

Furthermore if $z \in \underline{P}(x) \cap B_2\left(\xi(x), Kh\right)$ then

$$z - C_2 h^2 \frac{x - \xi(x)}{\|\xi(x) - x\|_2} \in \overline{M}_j \tag{20}$$

and if $z \in \overline{P}(x) \cap B_2\left(\xi(x), Kh\right)$

$$z + C_2 h^2 \frac{x - \xi(x)}{\|\xi(x) - x\|_2} \in \overline{M}_i. \tag{21}$$

Proof Let B_1 be the Euclidean closed ball centered at $\xi(x) - R\frac{x-\xi(x)}{\|x-\xi(x)\|_2}$ of radius R and B_2 be the Euclidean closed ball centered at $\xi(x) + R\frac{x-\xi(x)}{\|x-\xi(x)\|_2}$ of radius R. By Assumption **A3**, $B_1 \subset \overline{M}_j$ and $B_2 \subset \overline{M}_i$ (see details in Appendix C.1). Then, the Hausdorff distance between $B_2\left(\xi(x), Kh\right) \cap M_j$ and $B_2\left(\xi(x), Kh\right) \cap \underline{P}(x)$, and between $B_2\left(\xi(x), Kh\right) \cap M_i$ and $B_2\left(\xi(x), Kh\right) \cap \overline{P}(x)$, are both upper bounded by the Hausdorff distance between $\partial B_1 \cup \partial B_2$ intersected with $B_2\left(\xi(x), Kh\right)$ and the intersection with $B_2\left(\xi(x), Kh\right)$ of the hyperplane:

$$P(x) = \left\{z \in [0, 1]^d \text{ s.t. } \left\langle z, \frac{x - \xi(x)}{\|x - \xi(x)\|_2}\right\rangle = \left\langle \xi(x), \frac{x - \xi(x)}{\|x - \xi(x)\|_2}\right\rangle\right\}.$$

By symmetry, this distance is equal to the Hausdorff distance between $\partial B_1 \cap B_2\left(\xi(x), Kh\right)$ and $P(x) \cap B_2\left(\xi(x), Kh\right)$.
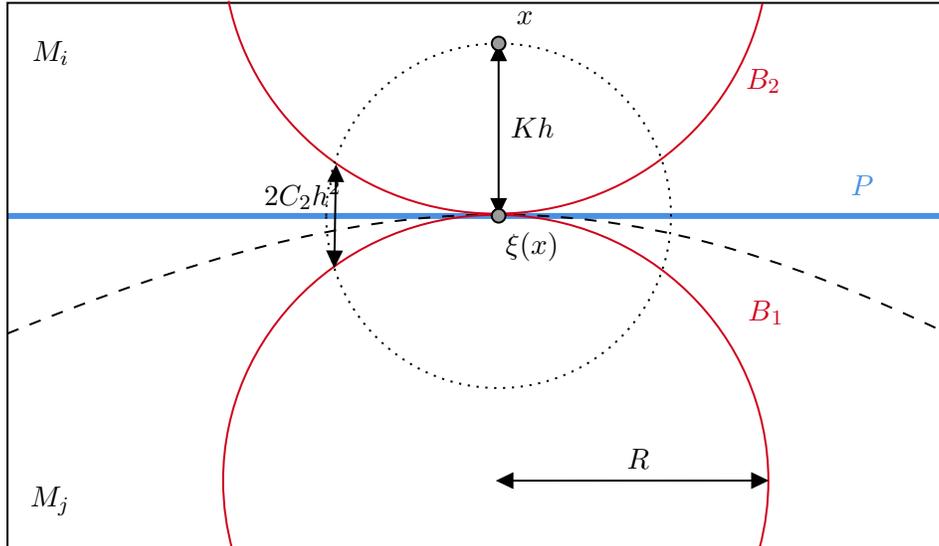
Figure 14: The tangent balls B_1 and B_2 of radius R delimit the region where $\partial M_i \cap \partial M_j$ lies in. 2D illustration.

Now, let $z \in \partial B_1 \setminus \{\xi(x)\}$, and $p(z)$ be its projection on $P(x)$. Let Q be the plane containing z, $p(z)$ and $\xi(x)$, Q intersects ∂B_1 in a circle $\mathcal{C}$ of radius R and intersects P in a line D tangent to $\mathcal{C}$. The problem then reduces to upper-bounding the distance between a circle and a tangent line around the intersection point. Without loss of generality, we can suppose that we are in $\mathbb{R}^2$, $\mathcal{C}$ is the circle of radius R centered at $(0, R)$ and D the line $y = 0$ (tangent to $\mathcal{C}$ at $(0,0)$). In $B((0,0), Kh)$, as $Kh < R/2$, $\mathcal{C}$ can be described as,

$$\mathcal{C} = \left\{ (x, y) \in B((0,0), Kh) \text{ s.t. } y = R - \sqrt{R^2 - x^2} \right\}.$$

Hence the distance between $\mathcal{C}$ and D in $B((0,0), Kh)$ is upper bounded by:

$$R - \sqrt{R^2 - (Kh)^2} = \frac{K^2}{2R} h^2 + O(h^3).$$

Assertions (18) and (19) then follow. Now, simply observe that since $Kh < R/2$, for all $z \in \underline{P}(x)$, $z - (R - \sqrt{R^2 - (Ch)^2})(x - \xi(x))/\|x - \xi(x)\|_2 \in B_1$ and (20) follows. And symmetrically, for all $z \in \overline{P}(x)$, $z + (R - \sqrt{R^2 + (Ch)^2})(x - \xi(x))/\|x - \xi(x)\|_2 \in B_2$ and (21) follows. ∎

Before turning to the full proof of Lemma 4, we give a high-level outline of the argument.

The idea being essentially the same for both (6) and (7), we present the outline for proving (6). Let $H_1 \in C_{\lambda, h}$ be a hypercube of center x_1 and $x \in H_1 \cap P_{\lambda + \sqrt{2}\sigma N_h, \sqrt{d}h}$:

- If the entire segment $[x, \xi(x)]$ is contained in H_1, then we directly have $[x, \xi(x)] \subset \widehat{\mathcal{F}}_\lambda$.

- Otherwise, let y be the first point along the segment $[x, \xi(x)]$ where it exits H_1. Then y lies in a hypercube $H_2 \in C_h$ of center x_2 and adjacent to H_1 (in the sense that they

share a common boundary point). Moving along the line segment $[x, \xi(x)]$, we go from a piece M_i, where f (around x) is significantly greater than λ to the boundaries of another piece M_j, where the signal f (around $\xi(x)$) is smaller than $\lambda + \varepsilon$, with $\varepsilon \asymp h^\alpha$. Exploiting Lemma 10, we show that the translation of the set $H_1 \cap \overline{M}_j \cap G_{1/N}$ by $x_2 - x_1$ (which is a subset of H_2), remains within $\overline{M}_j \cap G_{1/N}$, except for a subset of $H_1 \cap G_{1/N}$ that has cardinality of order $O(nh^{d+1})$. Using this and Assumptions **A0-A2**, we show that $H' \in \widehat{\mathcal{F}}_{\lambda + \varepsilon}$ for some $\varepsilon \asymp h^\alpha$.

- We then repeat the same argument starting from y. Iterating this reasoning along the segment $[x, \xi(x)]$, we establish assertion (6).

Proof [Proof of Lemma 4] We start by proving Assertion (6). Let $x \in \overline{M}_i \cap \widehat{\mathcal{F}}_\lambda \cap S_{\lambda + \sqrt{2}\sigma N_h h^\alpha, \sqrt{d}h}$ and assume that $\xi(x) \in \partial M_j$. In particular, we have $||x - \xi(x)|| \leq \sqrt{d}h$. Assume that n is sufficiently large such that $3\sqrt{d}h < R/2$. By Assumption **A3** (see Lemma 11 in Appendix C.1), we have:

$$([x, \xi(x)])^{\sqrt{d}h} \subset \overline{M}_i \cup \overline{M}_j.$$

Furthermore, as $x \in S_{\lambda + \sqrt{2}\sigma N_h h^\alpha, \sqrt{d}h}$,

$$x \in \overline{\left(M_j \cap \mathcal{F}_{\lambda + \sqrt{2}\sigma N_h h^\alpha} \right)}^{\sqrt{d}h}.$$

Let $H_1 \in C_{h, \lambda}$ be a hypercube containing x and denote x_1 its center. Suppose that there exists $y \in [x, \xi(x)]$ such that $y \notin H_1$. Denote H_2 the hypercube of C_h containing y and x_2 its center. Suppose furthermore that H_2 is adjacent to H_1 (i.e., $H_1 \cap H_2 \neq \emptyset$). If,

$$H_1 \cap M_i \cap \mathcal{F}_{\lambda + (\sqrt{2}\sigma N_h + 3L\sqrt{d})h^\alpha} \neq \emptyset$$

then, as $H_2 \subset H_1^{\sqrt{d}h}$, $H_2 \subset \mathcal{F}_{\lambda + (\sqrt{2}\sigma N_h + 5L\sqrt{d})h^\alpha}$ by Assumptions **A1** and **A2** (see Lemma 12 in Appendix C.2), and thus, by Lemma 7, $H_2 \subset \widehat{\mathcal{F}}_{\lambda + (2\sqrt{2}\sigma N_h + 5\sqrt{d})h^\alpha}$. From now on, we suppose:

$$H_1 \cap M_i \cap \mathcal{F}_{\lambda + (\sqrt{2}\sigma N_h + 3L\sqrt{d})h^\alpha} = \emptyset. \tag{22}$$

As $y \in H_2$, then,

$$\left\langle \frac{\xi(x) - x}{||\xi(x) - x||_2}, x_2 - x_1 \right\rangle = \left\langle \frac{y - x}{||y - x||_2}, x_2 - x_1 \right\rangle \geq 0. \tag{23}$$

Let us denote $\underline{P} = \underline{P}(x)$ and $P = P(x)$. Then, it follows that for all $z \in H_1 \cap \underline{P}$, $z + (x_2 - x_1) \in H_2 \cap \underline{P}$. Note that for all $z \in H_2 \cup H_1$, $||\xi(x) - z||_2 \leq 3\sqrt{d}h$. Thus, take $K = 3\sqrt{d}$ and let C_2 be the corresponding constant according to Lemma 10. For a set A and a vector u, we denote $A + u = \{z + u, z \in A\}$. By Lemma 10, if $z \in H_1 \cap \overline{M}_j \setminus P^{2C_2 h^2}$ then $z \in \underline{P}$. Thus, $z + (x_2 - x_1) \in \underline{P}$. Furthermore, if $z + (x_2 - x_1) \notin P^{2C_2 h^2}$, applying Lemma 10 again, we have that $z + (x_2 - x_1) \in \overline{M}_j$. Therefore, we have:

$$\left((H_1 \cap \overline{M}_j) \setminus P^{2C_2 h^2} + (x_2 - x_1) \right) \setminus P^{2C_2 h^2} \subset H_2 \cap \overline{M}_j. \tag{24}$$
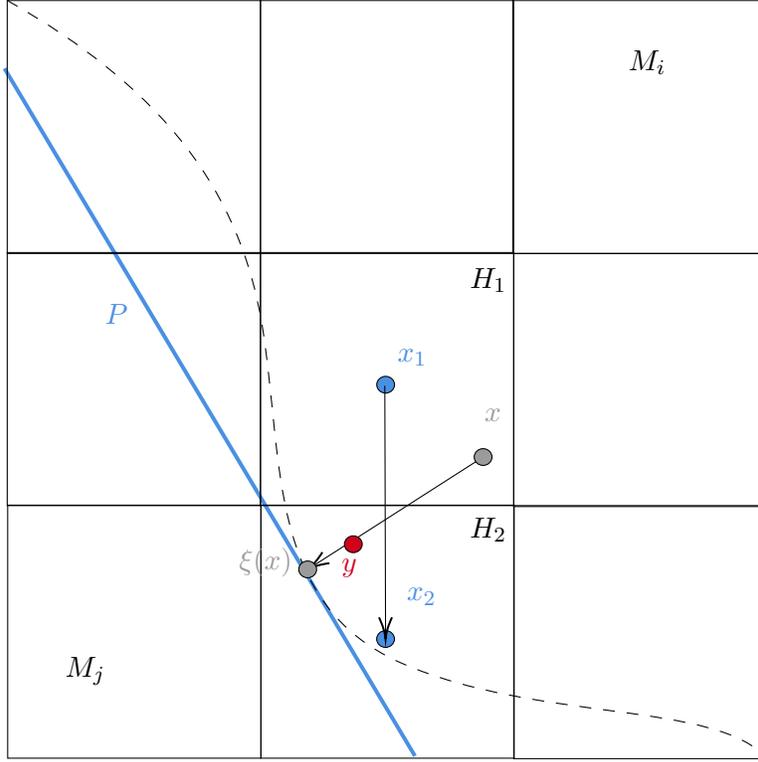
43

Figure 15: A 2D scenario where $\xi(x)$ is not in H_1.

As $H_2 \subset H_1^{\sqrt{d}h}$, Assumptions **A1** and **A2** imply that, for all $z \in H_2 \cap \overline{M}_j$, $z \in \mathcal{F}_{\lambda + (\sqrt{2}\sigma N_h + 3L\sqrt{d})h^\alpha}$ (see Lemma 12 in Appendix C.2). Hence, by (22),

$$\sup_{z \in H_2 \cap \overline{M}_j} f(z) \leq \inf_{z \in H_1 \cap M_i} f(z).$$

Now, observe that:

- if $z \in H_2 \cap \overline{M}_j$, either $z - (x_2 - x_1) \in M_i \cap H_1$, and then (22) ensures that $f(z) \leq f(z - (x_2 - x_1))$, or $z - (x_2 - x_1) \in \overline{M}_j \cap H_1$, and then Assumptions **A1** and **A2** ensure that $f(z) \leq f(z - (x_2 - x_1)) + L(\sqrt{d}h)^\alpha$ (as $||x_2 - x_1||_2 \leq \sqrt{d}h$ and by Lemma 12 in Appendix C.2). Thus, in both cases,

$$f(z) \leq f(z - (x_2 - x_1)) + L(\sqrt{d}h)^\alpha.$$

- If $z \in H_2 \cap M_i$ and $z - (x_2 - x_1) \in M_i \cap H_1$, then, Assumptions **A1** and **A2** ensure that $f(z) \leq f(z - (x_2 - x_1)) + L(\sqrt{d}h)^\alpha$ (Lemma 12 in Appendix C.2).

- If $z \in H_2 \cap M_i$ and $z - (x_2 - x_1) \in \overline{M}_j \cap H_1$, then, by (24), $z \in P^{2C_2h^2}$ or $z - (x_2 - x_1) \in P^{2C_2h^2}$.

Now, let $x_1, ..., x_n$ be the points of $G_{1/N}$ (the regular grid on which the signal is observed). Let $A_1 = H_2 \cap \overline{M}_j$, $A_2 = \{z \in H_2 \cap M_i \text{ s.t. } z - (x_2 - x_1) \in M_i \cap H_1\}$ and $A_3 = \{z \in$

$H_2 \cap M_i$ s.t. $z - (x_2 - x_1) \in \overline{M}_j \cap H_1\}$. As we have shown that:

$$A_3 \subset \{z \in H_2 \cap P^{2C_2 h^2}\} \cup \{z \in H_2 \text{ s.t. } z - (x_2 - x_1) \in H_1 \cap P^{2C_2 h^2}\}$$
$$= \left(P^{2C_2 h^2} \cup \left(P^{2C_2 h^2} + (x_2 - x_1)\right)\right) \cap H_2$$

there exists a constant κ (only depending on d and R) such that $|A_3 \cap G_{1/N}| \leq \kappa n h^{d+1}$. Using Assumption **A0**, it follows that:

$$\sum_{x_i \in H_2} f(x_i) = \sum_{x_i \in A_1} f(x_i) + \sum_{x_i \in A_2} f(x_i) + \sum_{x_i \in A_3} f(x_i)$$

$$\leq \sum_{x_i \in A_1} \left(f(x_i - (x_2 - x_1)) + L(\sqrt{d}h)^\alpha\right)$$

$$+ \sum_{x_i \in A_2} \left(f(x_i - (x_2 - x_1)) + L(\sqrt{d}h)^\alpha\right)$$

$$+ \sum_{x_i \in A_3} \left(f(x_i - (x_2 - x_1)) - f(x_i - (x_2 - x_1)) + f(x_i)\right)$$

$$\leq \sum_{x_i \in A_1 \cup A_2 \cup A_3} \left(f(x_i - (x_2 - x_1)) + L(\sqrt{d}h)^\alpha\right) + \sum_{x_i \in A_3} 2 \sup_{z \in [0,1]^d} |f(z)|$$

$$\leq \sum_{x_i \in A_1 \cup A_2 \cup A_3} \left(f(x_i - (x_2 - x_1)) + L(\sqrt{d}h)^\alpha\right) + 2n h^{d+1} \kappa M$$

$$= \sum_{x_i \in H_1} f(x_i) + n h^d L(\sqrt{d}h)^\alpha + 2n h^{d+1} \kappa M.$$

Now, as $H_1 \in C_{h,\lambda}$, recall that we have:

$$\frac{1}{n h^d} \sum_{x_i \in H_1} X_i = \frac{1}{n h^d} \sum_{x_i \in H_1} (f(x_i) + \sigma \varepsilon_i) \leq \lambda$$

Thus, by choice of h (and as $h \leq 1$),

$$\frac{1}{n h^d} \sum_{x_i \in H_2} X_i = \frac{1}{n h^d} \left(\sum_{x_i \in H_2} f(x_i) + \sigma \sum_{x_i \in H_2} \varepsilon_i\right)$$

$$\leq \frac{1}{n h^d} \left(\sum_{x_i \in H_1} f(x_i) + n h^d L(\sqrt{d}h)^\alpha + 2n h^{d+1} \kappa M + \sigma \sum_{x_i \in H_2} \varepsilon_i\right)$$

$$\leq \lambda + L(3\sqrt{d}h)^\alpha + 2\kappa M h + \frac{\sigma}{n h^d} \sum_{x_i \in H_2} \varepsilon_i - \frac{\sigma}{n h^d} \sum_{x_i \in H_1} \varepsilon_i$$

$$\leq \lambda + L(3\sqrt{d}h)^\alpha + 2\kappa M h^\alpha + 2 N_h \sqrt{2} \sigma \sqrt{\frac{\log(1/h^d)}{n h^d}}$$

$$\leq \lambda + L(3\sqrt{d}h)^\alpha + 2\kappa M h^\alpha + 2\sqrt{2} \sigma N_h h^\alpha.$$

Therefore:

$$H_2 \subset \widehat{\mathcal{F}}_{\lambda + (2\sqrt{2}\sigma N_h + 5L\sqrt{d} + 2\kappa M) h^\alpha}.$$

Now, if H_2 is not adjacent to H_1, there exists a finite sequence $H_3, H_4, ..., H_p$ of cube of C_h such that for all $k \in \{2, ..., n\}$, $[x, \xi(x)] \cap H_k \neq \emptyset$ and H_3 is adjacent to H_2, H_4 adjacent to H_3, ..., and H_p adjacent to H_1. Applying the previous reasoning iteratively then gives that, for all $k \in \{2, ..., p\}$,

$$H_k \subset \widehat{\mathcal{F}}_{\lambda+(1+p-k)(2\sqrt{2}\sigma N_h+5L\sqrt{d}+2\kappa M)h^\alpha}.$$

Note that since $||x - \xi(x)|| \leq \sqrt{d}h$, we have:

$$p \leq \left| B_2(x, \sqrt{d}h) \cap C_h \right| \leq \left| B_2(H_1, \sqrt{d}h) \cap C_h \right| \leq |B_\infty(H_1, dh) \cap C_h| \leq (2d)^d$$

. Thus, for all $k \in \{2, ..., n\}$,

$$H_k \subset \widehat{\mathcal{F}}_{\lambda+(1+(2d)^d)(2\sqrt{2}\sigma N_h+5L\sqrt{d}+2\kappa M)h^\alpha}.$$

and Assertion (6) follows.

Now, we prove assertion (7). The proof is essentially the same as that for assertion (6). Suppose that $x \in \widehat{\mathcal{F}}_\lambda \cap P_{\lambda,\sqrt{d}h} \cap \overline{M}_i$ and that $\gamma_{\lambda,\sqrt{d}h}(x) \in M_i$. In particular, it implies:

$$x \in \overline{\mathcal{F}_\lambda \cap M_i} \text{ and } ||x - \gamma_{\lambda,\sqrt{d}h}(x)||_2 \leq \sqrt{d}h.$$

Assume that n is sufficiently large such that $3\sqrt{d}h < R/2$. Assumption **A3** ensures (see Lemma 11 in Appendix C.1) that there exists $j \in \{1, ..., l\}$ such that

$$\left[x, \gamma_{\lambda,\sqrt{d}h}(x) \right]^{\sqrt{d}h} \subset \overline{M}_i \cup \overline{M}_j$$

Let $H_1 \in C_{h,\lambda}$ be a hypercube containing x and denote x_1 its center. Suppose that there exists $y \in \left[x, \gamma_{\lambda,\sqrt{d}h}(x) \right]$ such that $y \notin H_1$. Denote H_2 the hypercube of C_h containing y and x_2 its center. Suppose furthermore that H_2 is adjacent to H_1. If

$$H_1 \cap M_j \cap \mathcal{F}_{\lambda+(\sqrt{2}\sigma N_h+3L\sqrt{d})h^\alpha} \neq \emptyset$$

as $H_2 \subset H_1^{\sqrt{d}h}$, then $H_2 \subset \mathcal{F}_{\lambda+(\sqrt{2}\sigma N_h+5L\sqrt{d})h^\alpha}$ by Assumptions **A1** and **A2** (see Lemma 12 in Appendix C.2) and thus, by Lemma 7, $H_2 \subset \widehat{\mathcal{F}}_{\lambda+(2\sqrt{2}\sigma N_h+5\sqrt{d})h^\alpha}$. From now on, we suppose that:

$$H_1 \cap M_j \cap \mathcal{F}_{\lambda+(\sqrt{2}\sigma N_h+3L\sqrt{d})h^\alpha} = \emptyset. \tag{25}$$

As $y \in H_2$, we have:

$$\left\langle \frac{\gamma_{\lambda,\sqrt{d}h}(x) - x}{||\gamma_{\lambda,\sqrt{d}h}(x) - x||_2}, x_2 - x_1 \right\rangle = \left\langle \frac{y - x}{||y - x||_2}, x_2 - x_1 \right\rangle \geq 0. \tag{26}$$

Let us denote $\overline{P} = \overline{P}(\gamma_{\lambda,\sqrt{d}h}(x))$ and $P = P(\gamma_{\lambda,\sqrt{d}h}(x))$. Note that, by definition of $\gamma_{\lambda,\sqrt{d}h}$, $\overline{P}$ can be equivalently written as:

$$\overline{P} = \left\{ z \in [0,1]^d \text{ s.t. } \left\langle z - \xi(x), \frac{\gamma_{\lambda,\sqrt{d}h}(x) - x}{||\gamma_{\lambda,\sqrt{d}h}(x) - x||_2} \right\rangle \geq 0 \right\}.$$

Consequently, for all $z \in H_1 \cap \overline{P}$, $z + (x_2 - x_1) \in H_2 \cap \overline{P}$. Note that for all $z \in H_2 \cup H_1$,

$$||\xi(\gamma_{\lambda,\sqrt{dh}}(x)) - z||_2 = ||\xi(x) - z||_2 \leq 3\sqrt{dh}.$$

Thus, take $K = 3\sqrt{d}$ and let C_2 be the corresponding constant according to Lemma 10. By Lemma 10, if $z \in H_1 \cap \overline{M}_i \setminus P^{2C_2h^2}$ then $z \in \overline{P}$. Thus, $z + (x_2 - x_1) \in \overline{P}$. Furthermore, if $z + (x_2 - x_1) \notin P^{2C_2h^2}$, applying Lemma 10 again, we have that $z + (x_2 - x_1) \in \overline{M}_i$. Therefore, we have:

$$\left((H_1 \cap \overline{M}_i) \setminus P^{2C_2h^2} + (x_2 - x_1) \right) \setminus P^{2C_2h^2} \subset H_2 \cap \overline{M}_i. \tag{27}$$

As $H_2 \subset H_1^{\sqrt{dh}}$, Assumptions **A1** and **A2** implies that, for all $z \in H_2 \cap \overline{M}_i$, $z \in \mathcal{F}_{\lambda+3L\sqrt{dh}^\alpha}$ (see Lemma 12 in Appendix C.2). Hence, by (25),

$$\sup_{z \in H_2 \cap \overline{M}_i} f(z) \leq \inf_{z \in H_1 \cap M_j} f(z) \tag{28}$$

Now, observe that:

- if $z \in H_2 \cap \overline{M}_i$, either $z - (x_2 - x_1) \in M_j \cap H_1$ and (28) ensures that $f(z) \leq f(z - (x_2 - x_1))$, or $z - (x_2 - x_1) \in \overline{M}_i \cap H_1$ and, as $||x_1 - x_2||_2 \leq \sqrt{dh}$, Assumptions **A1** and **A2** ensure that $f(z) \leq f(z - (x_2 - x_1)) + L(\sqrt{dh})^\alpha$ (Lemma 12 in Appendix C.2). Thus, in both cases,

$$f(z) \leq f(z - (x_2 - x_1)) + L(\sqrt{dh})^\alpha.$$

- If $z \in H_2 \cap M_j$ and $z - (x_2 - x_1) \in M_j \cap H_1$, then Assumptions **A1** and **A2** ensure that $f(z) \leq f(z - (x_2 - x_1)) + L(\sqrt{dh})^\alpha$ (Lemma 12 in Appendix C.2).

- If $z \in H_2 \cap M_j$ and $z - (x_2 - x_1) \in \overline{M}_i \cap H_1$, then, by (27), $z \in P^{2C_2h^2}$ or $z - (x_2 - x_1) \in P^{2C_2h^2}$.

Now, let $x_1, ..., x_n$ be the points of $G_{1/N}$. Let $A_1 = H_2 \cap \overline{M}_i$, $A_2 = \{z \in H_2 \cap M_j$ s.t. $z - (x_2 - x_1) \in M_j \cap H_1\}$ and $A_3 = \{z \in H_2 \cap M_j$ s.t. $z - (x_2 - x_1) \in \overline{M}_i \cap H_1\}$. Again, there exists a constant κ (only depending on d and R) such that $|A_3 \cap G_{1/N}| \leq \kappa n h^{d+1}$. Using Assumption **A0**, it follows that:

$$\begin{aligned}
\sum_{x_i \in H_2} f(x_i) &= \sum_{x_i \in A_1} f(x_i) + \sum_{x_i \in A_2} f(x_i) + \sum_{x_i \in A_3} f(x_i) \\
&\leq \sum_{x_i \in A_1} \left(f(x_i - (x_2 - x_1)) + L(\sqrt{dh})^\alpha \right) \\
&\quad + \sum_{x_i \in A_2} \left(f(x_i - (x_2 - x_1)) + L(\sqrt{dh})^\alpha \right) \\
&\quad + \sum_{x_i \in A_3} (f(x_i - (x_2 - x_1)) - f(x_i - (x_2 - x_1)) + f(x_i)) \\
&\leq \sum_{x_i \in H_1} f(x_i) + n h^d L(\sqrt{dh})^\alpha + 2 n h^{d+1} \kappa M.
\end{aligned}$$

Now, as $H_1 \in C_{h,\lambda}$, recall that we have:

$$\frac{1}{nh^d} \sum_{x_i \in H_1} X_i = \frac{1}{nh^d} \sum_{x_i \in H_1} (f(x_i) + \sigma \varepsilon_i) \leq \lambda$$

Thus, by choice of h, for n sufficiently large such that $h < 1$,

$$\frac{1}{nh^d} \sum_{x_i \in H_2} X_i = \frac{1}{nh^d} \left(\sum_{x_i \in H_2} f(x_i) + \sigma \sum_{x_i \in H_2} \varepsilon_i \right)$$

$$\leq \frac{1}{nh^d} \left(\sum_{x_i \in H_1} f(x_i) + nh^d L(\sqrt{d}h)^\alpha + 2nh^{d+1}\kappa M + \sigma \sum_{x_i \in H_2} \varepsilon_i \right)$$

$$\leq \lambda + L(3\sqrt{d}h)^\alpha + 2\kappa M h + \frac{\sigma}{nh^d} \sum_{x_i \in H_2} \varepsilon_i - \frac{\sigma}{nh^d} \sum_{x_i \in H_1} \varepsilon_i$$

$$\leq \lambda + L(3\sqrt{d}h)^\alpha + 2\kappa M h^\alpha + 2N_h \sqrt{2} \sigma \sqrt{\frac{\log(1/h^d)}{nh^d}}$$

$$\leq \lambda + L(3\sqrt{d}h)^\alpha + 2\kappa M h^\alpha + 2\sqrt{2} \sigma N_h h^\alpha$$

$H_2 \subset \widehat{\mathcal{F}}_{\lambda + (2\sqrt{2}\sigma N_h + 5L\sqrt{d} + 2\kappa M)h^\alpha}$. Applying again the iterative reasoning used for assertion (6), we obtain assertion (7).

∎

B.7 Proof of Lemma 5

This section is dedicated to the proof of Lemma 5 from Section 3.

Proof Let $h > \frac{1}{N}$ and $H \subset [0,1]^d$ be a closed hypercube of side h. As the $(\varepsilon_i)_{i=1,\dots,n}$ are i.i.d and standard Gaussian variables, we have, for all $H \in C_h$,

$$\mathbb{P}\left(\left| \frac{1}{nh^d} \sum_{x_i \in H} \sigma \varepsilon_i \right| \geq t \right) \leq 2\exp\left(-\frac{nh^d t^2}{2\sigma^2} \right).$$

And thus, as the number of point in any $H \in C_h$ is at least to nh^d,

$$\mathbb{P}\left(\left| \frac{1}{nh^d} \sum_{x_i \in H} \sigma \varepsilon_i \right| \geq t \right) \leq 2\exp\left(-\frac{nh^d t^2}{2\sigma^2} \right).$$

Now, by union bound, using $|C_h| \leq (1/h)^d$,

$$\mathbb{P}\left(\max_{H \in C_h} \left| \frac{1}{nh^d} \sum_{x_i \in H} \sigma \varepsilon_i \right| \geq t \right) \leq 2\left(\frac{1}{h} \right)^d \exp\left(-\frac{nh^d t^2}{2\sigma^2} \right)$$

and thus,

$$\mathbb{P}\left(N_h \geq t\right) \leq 2 \left(\frac{1}{h}\right)^d \exp\left(-t^2 \log\left(1/h^d\right)\right).$$

Now, take $t \geq \sqrt{8}$, then $t^2/4 + 2 \leq t^2$. Thus, if $h < 1$

$$\mathbb{P}\left(N_h \geq t\right) \leq 2 \left(\frac{1}{h}\right)^d \exp\left(-\frac{1}{2}t^2 \log\left(1 + \frac{1}{h^d}\right)\right)$$

$$\leq 2 \left(\frac{1}{h}\right)^d \exp\left(-(t^2/8 + 1) \log\left(1 + \frac{1}{h^d}\right)\right)$$

$$\leq 2 \exp(-t^2 \log(2)/8).$$

Observe that, for all $t \leq \sqrt{8}$,

$$\exp(-t^2 \log(2)/8) \geq \exp(-\log(2))$$

and thus, for all $t \leq \sqrt{8}$,

$$2 \exp(\log(2)) \times \exp(-t^2 \log(2)/8) \geq 1 \geq \mathbb{P}\left(N_h \geq t\right).$$

It follows that, for all $t > 0$,

$$\mathbb{P}\left(N_h \geq t\right) \leq 2 \exp(\log(2)) \times \exp(-t^2 \log(2)/8).$$

∎

Appendix C. Claims Details

C.1 Lemma 11

This section provides details supporting a key claim that was repeatedly invoked in the previous proofs: namely, that Assumption **A3** implies that, locally, the boundaries of regular pieces separate at most two regions. We formalize this claim in the following lemma.

Lemma 11 *Let $x \in [0,1]^d$ and $h < R$. Under Assumption **A3**, there exists $1 \leq i, j \leq l$ such that $B_2(x, h) \subset \overline{M}_i \cap \overline{M}_j$.*

Proof Suppose, by contradiction, that $B_2(x, h)$ intersects three or more regular pieces. Then either there exists a multiple point $z \in B_2(x, h)$, that is, a point lying in the boundaries of at least three distinct regular pieces. Let $M_{i_1}, M_{i_2}, M_{i_3}$ be three such pieces, so that $z \in \partial M_{i_1} \cap \partial M_{i_2} \cap \partial M_{i_3}$. By Theorem 4.8 of Federer (1959), and under Assumption **A3**, there exist three Euclidean balls of radius $R/2$, denoted B_1, B_2, B_3, all containing z and such that $B_j \subset M_{i_j} \cup \{z\}$ for all $1 \leq j \leq 3$. In particular, $B_1 \cap B_2 \cap B_3 = \{z\}$, which is a contradiction, since no three balls (with strictly positive radii) in $\mathbb{R}^d$ can intersect at a unique point. This excludes the case of a multiple point. Now, suppose that there is no multiple point within $B_2(x, h)$. Then there exists a regular piece M_{i_1} such that

$$\partial M_{i_1} \cap \left(\bigcup_{j \neq i_1} \partial M_j \setminus \partial M_{i_1}\right) \cap B_2(x, h) = \emptyset,$$

but both $\partial M_{i_1} \cap B_2(x,h) \neq \emptyset$ and $\left(\bigcup_{j \neq i_1} \partial M_j \setminus \partial M_{i_1} \right) \cap B_2(x,h) \neq \emptyset$. Let

$$(y_1, y_2) \in \operatorname{argmin}_{y_1 \in \partial M_{i_1} \cap B_2(x,h),\, y_2 \in \left(\bigcup_{j \neq i_1} \partial M_j \setminus \partial M_{i_1} \right) \cap B_2(x,h)} \|y_1 - y_2\|_2,$$

Note that $\|y_1 - y_2\|_2 > 0$ and define $z = (y_1 + y_2)/2$. Since $B_2(x,h)$ is convex, $z \in B_2(x,h)$. If $z \in \bigcup_{j=1}^{l} \partial M_j$, then

$$d_2 \left(\partial M_{i_1}, \bigcup_{j \neq i_1} \partial M_j \setminus \partial M_{i_1} \right) \leq \frac{\|y_1 - y_2\|_2}{2} < \|y_1 - y_2\|_2,$$

which contradicts the minimality of $\|y_1 - y_2\|_2$. Therefore, using that $d_2(z, \partial M_{i_1}) \leq \|y_1 - y_2\|_2/2 \leq h$, we conclude that

$$z \in B_2 \left(\bigcup_{j=1}^{l} \partial M_j, h \right) \setminus \bigcup_{j=1}^{l} \partial M_j.$$

Now, the point z admits (at least) two distinct closest points in $\bigcup_{j=1}^{l} \partial M_j$, namely y_1 and y_2. If this were not the case, there would exist $y_3 \in \bigcup_{j=1}^{l} \partial M_j$ such that $\|z - y_3\|_2 < \|y_1 - y_2\|_2/2$, which would imply

$$d_2 \left(\partial M_{i_1}, \bigcup_{j \neq i_1} \partial M_j \setminus \partial M_{i_1} \right) \leq \frac{\|y_1 - y_2\|_2}{2} + \|z - y_3\|_2 < \|y_1 - y_2\|_2,$$

contradicting again the minimality of $\|y_1 - y_2\|_2$. Hence, z has at least two distinct closest points in $\bigcup_{j=1}^{l} \partial M_j$, which violates the reach condition from Assumption **A3**. This completes the argument. ∎

C.2 Lemma 12

This section provides details supporting another key claim that was repeatedly invoked in the previous proofs involving Assumptions **A1** and **A2**, formalized as the following lemma.

Lemma 12 *Let $i \in \{1, ..., l\}$, $\lambda \in \mathbb{R}$, $x \in \overline{M_i} \cap \mathcal{F}_\lambda$ and $h > 0$. Under Assumptions **A1** and **A2**, we have $B_2(x,h) \cap \overline{M_i} \subset \mathcal{F}_{\lambda + Lh^\alpha}$.*

Proof By Assumption **A1** for all $y \in B_2(x,h) \cap M_i$,

$$|f(x) - f(y)| \leq L\|x - y\|_2^\alpha \leq Lh^\alpha$$

Thus $B_2(x,h) \cap M_i \subset \mathcal{F}_{\lambda + Lh^\alpha}$. Moreover, if $z \in \partial M_i \cap B_2(x,h)$, there exists $(y_n)_{n \in \mathbb{N}}$ a sequence of elements of $B_2(x,h) \cap M_i$ converging to z. Then, by Assumption **A2**, we have:

$$f(z) \leq \lim_{n \to +\infty} f(y_n) \leq \lambda + Lh^\alpha$$

and consequently $B_2(x,h) \cap \overline{M_i} \subset \mathcal{F}_{\lambda + Lh^\alpha}$. ∎

Following the same reasoning, the result of Lemma 12 can also be extended, supposing only that $x \in \overline{M_i}$ and $\lim_{z \in M_i \to x} \leq \lambda$.

Appendix D. Extension to the Gaussian White Noise Model.

Beyond the nonparametric regression model considered in this work, our analysis can be readily adapted to other standard models. In particular, this applies to the Gaussian white noise model, described by the stochastic equation

$$dX_{t_1,...,t_d} = f(t_1, ..., t_d)\, dt_1 \cdots dt_d + \theta\, dW_{t_1,...,t_d},$$

where W is a d-parameter Wiener field, f is a signal in $S_d(M, L, \alpha, R)$, and $\theta \geq 0$ represents the noise level. Although this model may seem far from practical applications, it is an important theoretical framework due to its many connections with other, more data-oriented models (see, e.g., Tsybakov, 2008, Section 1.1). In this setting, we consider the sublevel set estimator:

$$\widehat{\mathcal{F}}_{\lambda,h} = \bigcup_{H \in C_{h,\lambda}} H \ , \text{ with } C_{h,\lambda} = \left\{ H \in C_h \text{ such that } \int_H dX - \int_H \lambda \leq 0 \right\},$$

with $h \asymp \left(\theta^2 \log \left(\frac{1}{\theta} \right) \right)^{\frac{1}{d+2\alpha}}$, and $\widehat{\text{dgm}}(f)$ the persistence diagram associated to the filtration $(\widehat{\mathcal{F}}_{\lambda,h})_{\lambda \in \mathbb{R}}$. Adapting the analysis of section 3, one can show that we have:

Theorem 4

$$\sup_{f \in S_d(M,L,\alpha,R)} \mathbb{E}\left(d_b\left(\widehat{\text{dgm}(f)}, \text{dgm}(f) \right) \right) \lesssim \left(\theta^2 \log \left(\frac{1}{\theta} \right) \right)^{\frac{\alpha}{d+2\alpha}}.$$

Furthermore, we can again show that these rates are minimax optimal:

Theorem 5

$$\inf_{\widehat{\text{dgm}}(f)} \sup_{f \in S_d(M,L,,\alpha,R)} \mathbb{E}\left(d_b\left(\widehat{\text{dgm}(f)}, \text{dgm}(f) \right) \right) \gtrsim \left(\theta^2 \log \left(\frac{1}{\theta} \right) \right)^{\frac{\alpha}{d+2\alpha}}.$$

It is worth noting that, making the standard choice $\theta = 1/\sqrt{n}$, the above rates coincide with those of Theorems 1 and 3.

References

Eddie Aamari and Clément Levrard. Non-asymptotic rates for manifold, tangent space, and curvature estimation. *Annals of Statistics*, 47, 2017. doi: 10.1214/18-AOS1685.

Eddie Aamari, Jisu Kim, Frédéric Chazal, Bertrand Michel, Alessandro Rinaldo, and Larry Wasserman. Estimating the reach of a manifold. *Electronic Journal of Statistics*, 13(1): 1359 – 1399, 2019. doi: 10.1214/19-EJS1551.

Robert Adler, Omer Bobrowski, Matthew Borman, Eliran Subag, and Shmuel Weinberger. Persistent homology for random fields and complexes. *Borrowing Strength: Theory Powering Applications*, 6, 2010. doi: 10.1214/10-IMSCOLL609.

Sivaraman Balakrishnan, Alesandro Rinaldo, Don Sheehy, Aarti Singh, and Larry Wasserman. Minimax rates for homology inference. In *Proceedings of the Fifteenth International Conference on Artificial Intelligence and Statistics*, volume 22 of *Proceedings of Machine Learning Research*, pages 64–72, 2012.

Clément Berenfeld, John Harvey, Marc Hoffmann, and Krishnan Shankar. Estimating the reach of a manifold via its convexity defect function. *Discrete & Computational Geometry*, 67(2):403–438, 2021. doi: 10.1007/s00454-021-00290-8.

Omer Bobrowski and Matthew Borman. Euler integration of gaussian random fields and persistent homology. *Journal of Topology and Analysis*, 4, 2012. doi: 10.1142/S1793525312500057.

Omer Bobrowski, Sayan Mukherjee, and Jonathan Taylor. Topological consistency via kernel estimation. *Bernoulli*, 23(1):288 – 328, 2017. doi: 10.3150/15-BEJ744.

Peter Bubenik. Statistical topological data analysis using persistence landscapes. *Journal of Machine Learning Research*, 16(1):77–102, 2015. ISSN 1532-4435.

Peter Bubenik and Peter Kim. A statistical approach to persistent homology. *Homology, Homotopy and Applications*, 9, 2006.

Peter Bubenik, Gunnar Carlsson, Peter Kim, and Zhiming Luo. Statistical topology via Morse theory persistence and nonparametric estimation. *Contemporary Mathematics*, 516:75–92, 2009. doi: 10.1090/conm/516/10167.

Frédéric Chazal and Vincent Divol. The Density of Expected Persistence Diagrams and its Kernel Based Estimation. In Bettina Speckmann and Csaba D. Tóth, editors, *34th International Symposium on Computational Geometry (SoCG 2018)*, volume 99 of *Leibniz International Proceedings in Informatics (LIPIcs)*, pages 26:1–26:15, Dagstuhl, Germany, 2018. Schloss Dagstuhl – Leibniz-Zentrum für Informatik. ISBN 978-3-95977-066-8. doi: 10.4230/LIPIcs.SoCG.2018.26.

Frédéric Chazal, David Cohen-Steiner, Marc Glisse, Leonidas Guibas, and Steve Oudot. Proximity of persistence modules and their diagrams. In *Proceedings of the Twenty-Fifth Annual Symposium on Computational Geometry*, SCG '09, page 237–246. Association for Computing Machinery, 2009. doi: 10.1145/1542362.1542407.

Frédéric Chazal, Leonidas Guibas, Steve Oudot, and Primoz Skraba. Persistence-based clustering in Riemannian manifolds. *Journal of the ACM*, 60(6), 2013. ISSN 0004-5411. doi: 10.1145/2535927.

Frédéric Chazal, Vin de Silva, Marc Glisse, and Steve Oudot. *The Structure and Stability of Persistence Modules*. SpringerBriefs in Mathematics. Springer Verlag, 2016. doi: 10.1007/978-3-319-42545-0.

Frédéric Chazal and Bertrand Michel. An introduction to topological data analysis: fundamental and practical aspects for data scientists, 2021. arXiv preprint, arXiv: 1710.04019.

Frédéric Chazal, David Cohen-Steiner, and André Lieutier. A sampling theory for compact sets in Euclidean space. *Discrete & Computational Geometry*, 41:461–479, 2006. doi: 10.1007/s00454-009-9144-8.

Frédéric Chazal, Leonidas Guibas, Steve Oudot, and Primoz Skraba. Scalar field analysis over point cloud data. *Discrete & Computational Geometry*, 46:743–775, 2011. doi: 10.1007/s00454-011-9360-x.

Frédéric Chazal, Marc Glisse, Catherine Labruère Chazal, and Bertrand Michel. Convergence rates for persistence diagram estimation in topological data analysis. *31st International Conference on Machine Learning, ICML 2014*, 1, 2014.

Moo Chung, Peter Bubenik, and Peter Kim. Persistence diagrams of cortical surface data. *Information processing in medical imaging : proceedings of the conference*, 21:386–97, 2009.

William Crawley-Boevey. Decomposition of pointwise finite-dimensional persistence modules, 2012. arXiv preprint, arXiv:1210.0819.

Vincent Divol and Théo Lacombe. Estimation and quantization of expected persistence diagrams. In *ICML*, volume 139 of *Proceedings of Machine Learning Research*, pages 2760–2770. PMLR, 2021.

Pawel Dlotko. Cubical complex. In *GUDHI User and Reference Manual*. GUDHI Editorial Board, 3.11.0 edition, 2025. URL `https://gudhi.inria.fr/doc/3.11.0/group__cubical__complex.html`.

Paweł Dłotko and Thomas Wanner. Rigorous cubical approximation and persistent homology of continuous functions. *Computers & Mathematics with Applications*, 75(5): 1648–1666, 2018. ISSN 0898-1221. doi: https://doi.org/10.1016/j.camwa.2017.11.027.

Herbert Edelsbrunner and John Harer. Persistent homology—a survey. *Discrete & Computational Geometry - DCG*, 453, 2008. doi: 10.1090/conm/453/08802.

Brittany Fasy, Fabrizio Lecci, Alessandro Rinaldo, Larry Wasserman, Sivaraman Balakrishnan, and Aarti Singh. Confidence sets for persistence diagrams. *The Annals of Statistics*, 42:2301–2339, 2014. doi: 10.1214/14-AOS1252.

Herbert Federer. Curvature measures. *Transactions of the American Mathematical Society*, 1959.

Christopher Genovese, Marco Perone-Pacifico, Isabella Verdinelli, and Larry Wasserman. Minimax manifold estimation. *Journal of Machine Learning Research*, 13(43):1263–1291, 2012.

GUDHI. *GUDHI User and Reference Manual*. GUDHI Editorial Board, 3.11.0 edition, 2025. URL `https://gudhi.inria.fr/doc/3.11.0/`.

Allen Hatcher. *Algebraic topology*. Cambridge University Press, Cambridge, 2000.

Yasuaki Hiraoka, Tomoyuki Shirai, and Khanh Duy Trinh. Limit theorems for persistence diagrams. *Annals of Applied Probability*, 28, 2016. doi: 10.1214/17-AAP1371.

Jonathan Jaquette and Miroslav Kramár. On ε approximations of persistence diagrams. *Mathematics of Computation*, 86:1, 2015. doi: 10.1090/mcom/3137.

Matthew Kahle. Random geometric complexes. *Discrete & Computational Geometry*, 45: 553–573, 2009.

Shizuo Kaji, Takeki Sudo, and Kazushi Ahara. Cubical ripser: Software for computing persistent homology of image and volume data, 2020. arXiv preprint, arXiv:2005.12692.

Jisu Kim, Alessandro Rinaldo, and Larry Wasserman. Minimax rates for estimating the dimension of a manifold. *Journal of Fourier Analysis and Applications*, 2016.

Jisu Kim, Jaehyeok Shin, Frédéric Chazal, Alessandro Rinaldo, and Larry Wasserman. Homotopy reconstruction via the cech complex and the vietoris-rips complex, 2020. arXiv preprint, arXiv:1903.06955.

Johannes Krebs. On limit theorems for persistent betti numbers from dependent data. *Stochastic Processes and their Applications*, 139:139–174, 2021. ISSN 0304-4149. doi: https://doi.org/10.1016/j.spa.2021.04.013.

Johannes Krebs and Christian Hirsch. Functional central limit theorems for persistent betti numbers on cylindrical networks. *Scandinavian Journal of Statistics*, 49:427 – 454, 2020.

Johannes Krebs and Wolfgang Polonik. On the asymptotic normality of persistent betti numbers. *Advances in Applied Probability*, 57(2):492–523, 2025. doi: 10.1017/apr.2024.61.

Hosein Masoomy, Behrouz Askari, Mortezza Najafi, and Seyed Movahed. Persistent homology of fractional gaussian noise. *Physical Review E*, 104, 2021. doi: 10.1103/PhysRevE.104.034116.

Partha Niyogi, Stephen Smale, and Shmuel Weinberger. Finding the homology of submanifolds with high confidence from random samples. *Discrete & Computational Geometry*, 39:419–441, 2008. doi: 10.1007/s00454-008-9053-2.

Nina Otter, Mason Porter, Ulrike Tillmann, Peter Grindrod, and Heather Harrington. A roadmap for the computation of persistent homology. *Epj Data Science*, 6, 2017.

Takashi Owada. Convergence of persistence diagram in the sparse regime. *The Annals of Applied Probability*, 32(6):4706 – 4736, 2022. doi: 10.1214/22-AAP1800.

Daniel Perez. On the persistent homology of almost surely c0 stochastic processes. *Journal of Applied and Computational Topology*, 7:879–906, 2020.

Daniel Perez. *Persistent homology of stochastic processes and their zeta functions*. PhD thesis, Université Paris-Saclay, 2022a.

Daniel Perez. ζ-functions and the topology of superlevel sets of stochastic processes, 2022b. arXiv preprint, arXiv:2110.10982.

Pratyush Pranav. Topology and geometry of gaussian random fields ii: on critical points, excursion sets, and persistent homology, 2021. arXiv preprint, arXiv:2109.08721.

Pratyush Pranav, Rien van de Weygaert, Gert Vegter, Bernard Jones, Robert Adler, Job Feldbrugge, Changbom Park, Thomas Buchert, and Michael Kerber. Topology and geometry of gaussian random fields i: on Betti numbers, Euler characteristic, and Minkowski functionals. *Monthly Notices of the Royal Astronomical Society*, 485(3):4167–4208, 2019. ISSN 0035-8711. doi: 10.1093/mnras/stz541.

Peihua Qiu. *Image Processing and Jump Regression Analysis*. Wiley, 2005.

Andrew Thomas. Convergence of persistence diagrams for discrete time stationary processes. *Journal of Applied and Computational Topology*, 9, 2024. URL `https://api.semanticscholar.org/CorpusID:271088477`.

Alexandre Tsybakov. *Introduction to Nonparametric Estimation*. Springer Publishing Company, Incorporated, 2008.

Renata Turkeš, Jannes Nys, Tim Verdonck, and Steven Latré. Noise robustness of persistent homology on greyscale images, across filtrations and signatures. *PLOS ONE*, 16(9):1–26, 2021. doi: 10.1371/journal.pone.0257215.

Hubert Wagner, Chao Chen, and Erald Vuçini. *Efficient Computation of Persistent Homology for Cubical Data*, pages 91–106. Springer Berlin Heidelberg, Berlin, Heidelberg, 2012. ISBN 978-3-642-23175-9. doi: 10.1007/978-3-642-23175-9_7. URL `https://doi.org/10.1007/978-3-642-23175-9_7`.

D. Yogeshwaran and Robert Adler. On the topology of random complexes built over stationary point processes. *The Annals of Applied Probability*, 25, 2012. doi: 10.1214/14-AAP1075.